Deliverable Report

Deliverable Title:

Report with the results of the laboratory trials with partially recycled alloys

Deliverable No.	Deliverable 1.3
Deliverable nature	Report
Work Package (WP)	WP 1
Task	Task 1.3
Dissemination level [1]	Public
Number of pages	57
Keywords	Critical raw materials, aluminium scrap, chemical composition, analysis, microstructure, mechanical properties
Authors	Manel da Silva, Jaume Pujante (EUT)
Contributors	Sonia Boczkal (IMN)
Due date of deliverable	31.01.2022
Actual submission date	07.04.2022

Technical References

Project acronym	SALEMA
Project full title	Substitution of Critical Raw Materials on Aluminium Alloys for electrical vehicles
Call	H2020-SC5-2020-2
Grant number	101003785
Project website	salemaproject.eu
Coordinator	Fundacion Eurecat

[1] PU = Public
PP = Restricted to other programme participants (including the Commission Services)
RE = Restricted to a group specified by the consortium (including the Commission Services)
CO = Confidential, only for members of the consortium (including the Commission Services)

The project has received funding from the European Union's Horizon 2020 research and innovation programme under grant agreement No 101003785

Document history

V	Date	Author (Affiliation)	Actions& Approvals
V1.0	16.02.2022	Manel da Silva (EUT)	Template filled up with section titles and rough content proposal.
V2.0	01.04.2022	Jaume Pujante (EUT)	Provision of additional lab results
V3.0	06.04.2022	Manel da Silva (EUT)	Finalisation

Summary

Deliverable 1.3 summarizes the main results achieved in Task 1.3 for the development of the new partially recycled alloys.

The document presents the experimental tests conducted to evaluate the impact that have the use of scrap in the properties of aluminium alloys. A total of 6 aluminium alloys, intended for the 3 processes of SALEMA project, have been evaluated for different scrap ratios (0, 10, 40, 60, 80 and 100%).

The characteristics evaluated for each alloy varied slightly according to their corresponding forming process, but, in general it was evaluated: quantity and type of inclusions and general microstructure, formability and mechanical properties.

In general, the results show an increment on the number of inclusions with the percentage of scrap and a decrease in the alloy flowability for HPDC alloys. However, no relevant impact has been observed on the alloy mechanical properties under the current experimental conditions used.

The project has received funding from the European Union's Horizon 2020 research and innovation programme under grant agreement No 101003785

Disclaimer

This publication reflects only the author's view. The Agency and the European Commission are not responsible for any use that may be made of the information it contains.

Abbreviations

Abbreviation / Acronyms	Description
HPDC	High-Pressure Die Casting
LM	Light Microscope
SEM	Scanning Emission Microscope

Table of contents

The project has received funding from the European Union's Horizon 2020 research and innovation programme under grant agreement No 101003785

List of tables

List of figures

The project has received funding from the European Union's Horizon 2020 research and innovation programme under grant agreement No 101003785

The project has received funding from the European Union's Horizon 2020 research and innovation programme under grant agreement No 101003785

1. Introduction and Background

One of the main objectives of the SALEMA project is to develop new, high-performance, partially recycled aluminium alloys for electric vehicles. In other words, the feedstock of these alloys shall partially consist of secondary aluminium alloys recycled from well-identified scrap sources. WP1 sets the basis for the development of those new, high-performance alloys.

1.1. Objectives of task and deliverable

Within WP1, Task 1.3 has the objective to evaluate the impact of using well sorted, but untreated scrap to produce SALEMA partially recycled alloys. The deliverable of Task 1.3 contains technical results about:

1. The research conducted on HPDC alloys evaluating chemical composition, flowability, type and quantity of inclusions, microstructure and tensile properties.
2. The research conducted on extrusion alloy 6063 evaluating chemical composition, type and quantity of inclusions, microstructure and tensile and compression properties.
3. The research conducted on stamping alloys evaluating chemical composition, microstructure of reference laminated material and cast material before and after deformation and hardness.

2. Laboratory trials with HPDC alloys

2.1. Experimental methodology

For each processing technology: HPDC, extrusion and stamping, 2 alloys were tested, producing specimens for material characterization with different level of scrap: 0, 20, 40, 60, 80 and 100 %. In order to combine several of these tests in one single trial journey, was used the approach of starting with 100 % of reference alloy or 100 % of scrap and adding the other component, first to a concentration of 20 % and in a second step to a concentration of 40 %.

For the tests with the HPDC alloys, the furnace (Figure 1) was charged with about 24,4 kg of one of the materials, either ingot of AlSi10MnMg alloy or of scrap, and heated up to a temperature of 710 ± 10ºC. Three different sample types were casted from the melt: 3 square plates (Figure 4), 3 small ingots (Figure 5) and 1 fluidity test specimen (Figure 6).

Figure 1. Stotek furnace, with a crucible with a capacity of 50 kg of aluminium, used to melt the material of WP1 tests

The project has received funding from the European Union's Horizon 2020 research and innovation programme under grant agreement No 101003785

2.1.1. Feedstock materials used for the trials

Alloys and material format supplied by Raffmetal

The reference material used for the initial development of SALEMA HPDC alloys where billets produced by Raffmetal, in the format that they provide them to their customers, of AlSi10MnMg alloy (Figure 2). Raffmetal produced and delivered ingots from 3 different batches, produced with different level of Mg: about 0.2 %, about 0.3 % and about 0.45 %. The actual chemical composition measured by Raffmetal for the 3 Mg level is presented in ANNEX 1.

Figure 2. Image of the ingots supplied by Raffmetal for WP1 trials related to HPDC alloys

The chemical composition of a piece of a billet of each batch was also measured by Eurecat, in order to have a second measurement with the same equipment and procedure used for measuring the casting samples. In Table 1 are presented the chemical analysis obtained by arc/spark optical emission spectroscopy with Eurecat SPECTROMAXx spectrometer. The equipment and experimental procedure were already presented in detail in Deliverable 1.2. The same equipment and procedure were also used to measure the chemical compositions of the cast parts and the rest of compositions reported in this document.

n=5	%Si	% Fe	%Cu	%Mn	%Mg	%Zn	%Cr	%Ni	%Pb	%Sn	%Ti
AlSi10MnMg0.2	10.40	0.16	0.03	0.65	0.18	<0.01	<0.01	<0.01	<0.01	<0.01	0.07
AlSi10MnMg0.3	9.84	0.16	0.01	0.54	0.29	<0.01	<0.01	<0.01	<0.01	<0.01	0.06
AlSi10MnMg0.45	9.36	0.17	0.02	0.49	0.42	0.01	<0.01	<0.01	<0.01	<0.01	0.07

Table 1. Chemical composition measured at Eurecat for the 3 samples taken from each reference alloys lots provided by Raffmetal

Scrap used to mix with reference alloy

After reviewing together with COMET the lack of aluminium casting alloys with low impurities level (mainly, Fe, Cu and Zn) in their Zorba stream, it was decided to use an alternative scrap. Raffmetal supplied a casting scrap that was supposed to be homogeneous AlSi10MnMg scrap composed by casting sprues and defective components. Raffmetal supplied about 100 kg of this scrap in one big bag (Figure 3 a). However, a visual analysis, revealed some parts that seemed to have been produced by

The project has received funding from the European Union's Horizon 2020 research and innovation programme under grant agreement No 101003785

Gravity Casting and no by HPDC. An example is shown in Figure 3 b, where it can be observed one typical Permanent Mould Casting (PMC) sprue with its filter (left component of the right image).

Figure 3: General image of the foundry scrap provided by Raffmetal (left) and image of 3 parts selected to conduct a chemical analysis by spectrometry (right)

The 3 parts from Figure 3 b, as a representative selection of the different types of components and sprues, were analysed by Spark Plasma Analysis. The results of the analysed parts are presented in Table 2.

n=5	%Si	% Fe	%Cu	%Mn	%Mg	%Zn	%Ni	%Cr	%Pb	%Sn	%Ti
Spec 1	10.07	0.14	0.02	0.60	0.19	0.01	<0,01	<0,01	<0,01	<0,01	0.07
Spec 2	6.91	0.10	<0.01	0.01	0.36	<0.01	<0.01	<0.01	<0.01	<0.01	0.13
Spec 3	11.55	0.16	<0.01	0.65	0.33	<0.01	<0.01	<0.01	<0.01	<0.01	0.01

Table 2: Chemical composition measured by spark OES with SPECTROMAXx equipment on the 3 fragments selected from the AlSi10MnMg scrap supplied by Raffmetal

The analysis confirms the presence of parts of AlSi7Mg mixed up with the rest of primary HPDC parts of AlSi10MnMg alloy. As those parts can be easily identified visually, there were excluded for the trials, using just scrap of AlSi10MnMg alloy.

2.1.2. Moulds used and specimens extracted

Three different parts were cast for each material combination:

1. Square plate of 150 x 150 mm. The thickness of the plates depends on the amount of molten metal poured into de mould, but usually was about 25 mm. These parts were used to characterize the properties of the different alloy combination, extracting from them tensile specimens, metallographic samples and using them to analyse the chemical composition of the batch.

The project has received funding from the European Union's Horizon 2020 research and innovation programme under grant agreement No 101003785

Figure 4. Images of the mould used to cast 150 x 150 x 25 square plates and one of the cast specimens

2. Small ingots of about 1.5 kg each were casted in an ingot mould, by filling one of the cavities, prior to reaching the ingot neck. The approximate dimensions of the cast ingots were about 240x90x45. The ingots were cast to be sent to IMN to perform the Prefil Footprinter® tests and the compression tests for the extrusion alloys.

Figure 5. Images of the ingot mould used and one of the ingots cast

3. Additionally, to the cast samples obtained with the 2 previous moulds, the HPDC casting alloys, were also poured into the fluidity test mould (Figure 6). The geometry of mould was presented in Deliverable 1.1.

Figure 6. Pictures of the mould used for the fluidity test of the casting alloys and some of the samples obtained

The project has received funding from the European Union's Horizon 2020 research and innovation programme under grant agreement No 101003785

2.1.3. Experimental techniques

In addition to the determination of the chemical composition of the samples by optical spectrometry, the microstructural analysis and the tensile tests, already presented in Deliverable 1.1 and 1.2 in the present evaluation was used the Prefil Footprinter® to characterize the amount and type of inclusions present in the different materials.

The PREFIL (Figure 7) instrument is based on the pressure filtration principle. A ready-to-use crucible, equipped with a porous filter disc at the bottom, is first pre-heated and is installed in the pressure chamber. Then take a sample of liquid metal with a ladle, pours it into the crucible, and start the test. During the test, the system continuously weighs the metal in the weigh lade and displays curve of the accumulated weight versus the elapsed time. The cleaner the metal samples, the faster the curve rises. Optionally, the metal residue above the filter can be saved. A thorough off-line metallographic examination of the material trapped by the filter can confirm the results and extend the interpretation.

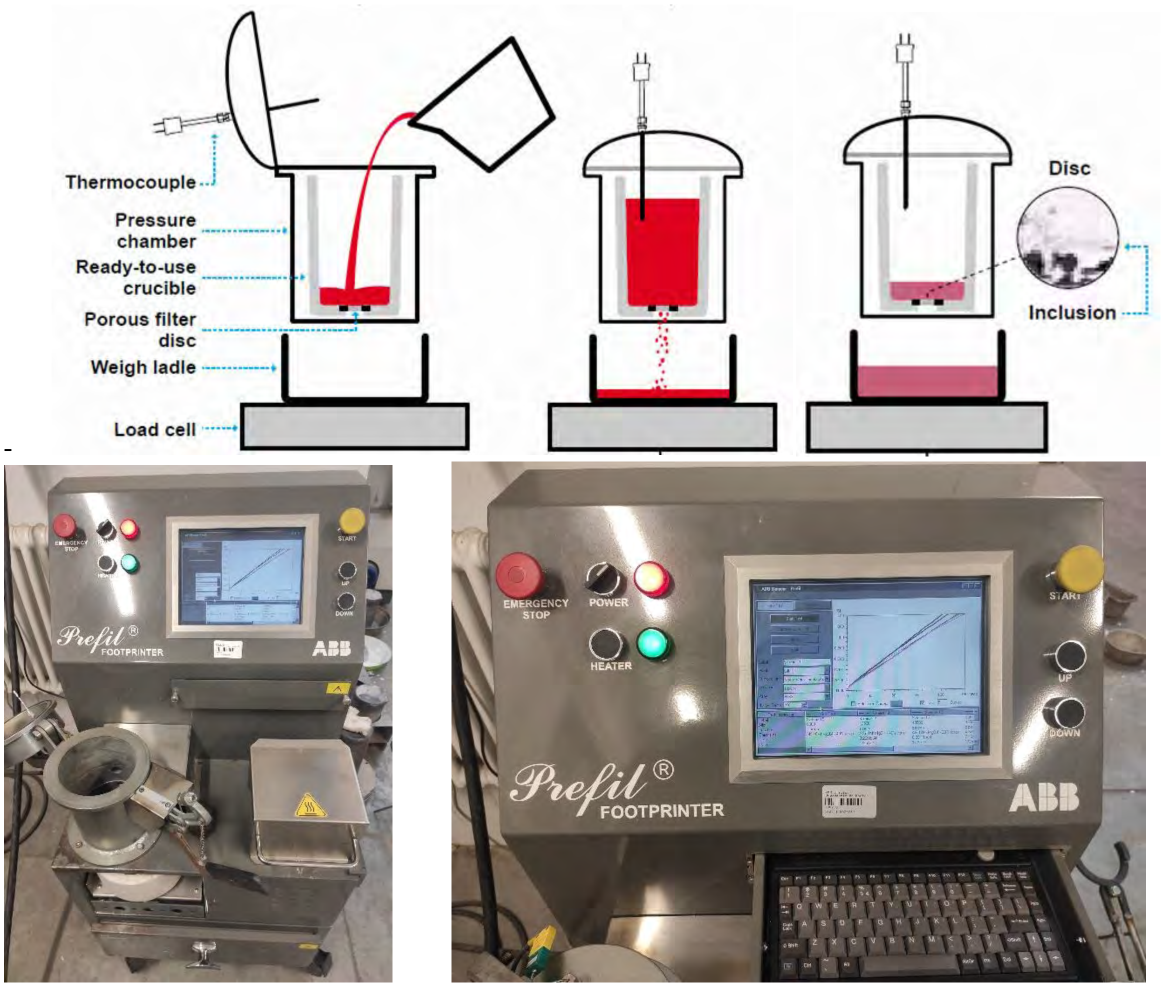

b.

Figure 7. Sampling scheme for analyzing inclusions (a.) and PREFIL apparatus (b.)

The material for analysis was melted in the induction coil (Figure 8). Crucible capacity approx. 2,5 kg. After remelting and obtaining the temperature of 730-740^{0}C, a sample was taken into the Prefil crucible. The test began after that temperature was obtained 700^{0}C.

The project has received funding from the European Union's Horizon 2020 research and innovation programme under grant agreement No 101003785

Figure 8. Induction coil with crucible

Figure 9. The samples prepared for LM and SEM

The samples with filter from Prefil device were cut, ground and polished (*Figure 9*). Metallographic examinations were observed on light microscopy (LM) Zeiss Axio Observer and scanning electron microscope (SEM) Inspect F50 with EDS EDAX chemical analysis in microareas (Fig. 6.).

The content of the inclusions concentrated on the surface of the test filter is then quantified using image analysis software. The quantitative analysis of inclusions was carried out on LM and SEM pictures with a total area of 0.6 mm^2 for each sample. This is then normalised by both nominal chord length, and by the mass of metal filtered, to give the familiar units of mm^2/kg. Inclusions are classified arbitrarily about the class and content (in mm^2/kg) (Table 3) [1].

Table 3: *Inclusion classifications [1]*

Class	Inclusion content, mm^2/kg
Very Light – (1)	0.0 – 0.05
Light – (2)	0.05 – 0.1
Moderate – (3)	0.1 – 0.4
Heavy – (4)	0.4 – 1.2
Excessive – (5)	≥1.2

The project has received funding from the European Union's Horizon 2020 research and innovation programme under grant agreement No 101003785

Figure 10. LM and SEM in Ł-IMN

2.2. Results obtained from the produced samples

2.2.1. Chemical composition of the different batches

As described in the experimental methodology section, the alloys used in this task to develop the HPDC alloys are AlSi10MnMg alloys with 3 different Mg levels. These alloys were combined with AlSi10MnMg selected scrap in different percentages, in steps of 20 %, from 0 % to 100 % scrap. The first alloy tested was the alloy with an intermediate level of Mg of about 0.3%. The chemical composition of the different samples extracted were measured and are presented in Table 4.

n=5	%Si	% Fe	%Cu	%Mn	%Mg	%Cr	%Ni	%Zn	%Ti
Mg0.3	10.06	0.22	0.17	0.49	0.30	<0.03	<0,03	0.06	0.03
Mg0.3-20%scrap	9.85	0.20	0.12	0.49	0.28	<0.03	<0,03	0.04	0.04
Mg0.3-40%scrap	9.97	0.19	0.10	0.50	0.28	<0.03	<0,03	0.04	0.04
Mg0.3-60%scrap	9.92	0.16	0.01	0.52	0.28	<0.03	<0,03	<0,03	0.05
Mg0.3-80%scrap	9.78	0.15	0.01	0.51	0.27	<0.03	<0,03	<0,03	0.05
100 % scrap	10.01	0.14	0.01	0.51	0.25	<0.03	<0,03	<0,03	0.06
EN AB-43500	9-11.5	<0.20	<0.03	0.4-0.8	0.15-0.6	<0.03	<0,03	<0.07	<0.15

Table 4: Chemical composition measured on the inspected plate for the different levels of scrap with the AlSi10MnMg0.3 alloy variant

In the results reported it is observed that the highest level of impurities belongs to the samples cast with the pure alloy. The level of Fe and Cu are higher than the actual upper limit of the standard for EN AB-43500 alloy. The concentration of those impurities in the samples, actually decreased when scrap was added.

Both elements, have also a higher concentration than the level measured in the specimens extracted from the original ingots (Table 1), which suggest that the higher level of impurities was due to an external contamination. Considering that the 3 first measures correspond to the first batch produced with AlSi10MnMg alloy, it is likely, that the reason of such contamination, was the presence of rests of a different alloy in the furnace.

In Table 5 are presented the results obtained with the alloy variant with the lower Mg content. It can be observed that the chemical composition remains mostly constant. The only clear trend is in the amount of Mg, that increases with the addition of scrap, as the scrap is richer in Mg than this alloy variant.

The project has received funding from the European Union's Horizon 2020 research and innovation programme under grant agreement No 101003785

n=5	%Si	% Fe	%Cu	%Mn	%Mg	%Cr	%Ni	%Zn	%Ti
Mg0.2	10.34	0.17	0.03	0.58	0.18	<0.03	<0,03	<0,03	0.06
Mg0.2-20%scrap	10.29	0.16	0.02	0.58	0.18	<0.03	<0,03	<0,03	0.06
Mg0.2-40%scrap	10.25	0.16	0.02	0.56	0.19	<0.03	<0,03	<0,03	0.06
Mg0.2-60%scrap	10.1	0.16	0.02	0.53	0.21	<0.03	<0,03	<0,03	0.06
Mg0.2-80%scrap	10.22	0.17	0.02	0.54	0.23	<0.03	<0,03	<0,03	0.06
EN AB-43500	9-11.5	<0.20	<0.03	0.4-0.8	0.15-0.6	<0.03	<0,03	<0.07	<0.15

Table 5: Chemical composition measured on the inspected plate for the different levels of scrap with the AlSi10MnMg0.2 alloy variant

In Table 6 are presented the chemical composition measured in the plates for the AlSi10MnMg alloy variant with the higher Mg content. In this case, only a single batch was produced, with the lowest scrap content, as the behaviour of those with higher amount of scrap, would be very similar to those obtained for the other alloy variants.

n=5	%Si	% Fe	%Cu	%Mn	%Mg	%Cr	%Ni	%Zn	%Ti
Mg0.45	9.42	0.17	0.02	0.45	0.41	<0.03	<0,03	<0,03	0.06
Mg0.45-20%scrap	9.45	0.17	0.02	0.58	0.18	<0.03	<0,03	<0,03	0.06
Mg0.45-40%scrap	10.25	0.16	0.02	0.56	0.19	<0.03	<0,03	<0,03	0.06
EN AB-43500	9-11.5	<0.20	<0.03	0.4-0.8	0.15-0.6	<0.03	<0,03	<0.07	<0.15

Table 6: Chemical composition measured on the inspected plate for the different levels of scrap with the AlSi10MnMg0.45 alloy variant

2.2.2. Fluidity test

The length of the different samples obtained with the fluidity test for the different HPDC alloys are presented in Table 7.

Material	1 mm	3 mm	5 mm	7 mm	9 mm	11 mm	Average
AlSi10MnMg0.2	0	135	35	135	60	85	75.00
AlSi10MnMg0.2 + 20% scrap	0	100	55	110	95	70	71.67
AlSi10MnMg0.2 + 40% scrap	0	90	40	80	65	60	55.83
AlSi10MnMg0.2 + 60% scrap	0	130	30	105	75	20	60.00
AlSi10MnMg0.2 + 80% scrap	0	40	5	70	20	0	22.50
100 % AlSi10MnMg scrap	0	70	5	75	20	10	30.00
AlSi10MnMg0.3	0	0	5	20	0	0	4.17
AlSi10MnMg0.3 + 20% scrap	0	35	5	55	0	25	20.00
AlSi10MnMg0.3 + 40% scrap	0	30	20	60	0	10	20.00
AlSi10MnMg0.3 + 60% scrap	0	10	30	40	0	0	13.33
AlSi10MnMg0.3 + 80% scrap	0	75	5	70	30	10	31.67
AlSi10MnMg0.45	0	85	20	80	50	40	45.83
AlSi10MnMg0.45 + 20% scrap	0	40	15	65	15	20	25.83
AlSi10MnMg0.45 + 40% scrap	0	40	5	45	10	0	16.67

Table 7: Length of the metal flow for the different channel sections of the fluidity test mould and final average fluidity value

It can be observed that, in general, the materials obtained with a higher amount of scrap show lower fluidity than the pure alloys or those with lower scrap content. It also seems that higher magnesium contents lead to lower flowability, being the alloy with an 0.2 of Mg concentration, the one with the

The project has received funding from the European Union's Horizon 2020 research and innovation programme under grant agreement No 101003785

highest flowability. In general, the metal flows better in the right side of the mould (3, 7 and 9 mm thick channels) than in the left side of the mould (1, 5 and 11).

2.2.3. Inclusion analysis with Prefil Footprinter®

In the following pages the results obtained with the Prefil Footprinter® are presented for the HPDC alloys. For each set of alloys with different Mg concentrations are presented a table summarising the main information of the test, curves with the material filtration kinetics, a graph comparing the filtering rate of the different tested samples, some images of the inclusions present over the filter, a table summarising the metallographic analysis of the particles and a histogram comparing the content of particles observed for each sample.

EN AC 43500 (~0,2 % Mg)

Table 8 summarizes the main results of the Prefil Footprinter® test. It can be observed that the filtering rate decreases with the amount of scrap used to produce the alloy and, consequently, the duration of the test increases. In Figure 11 are compared the filtration kinetics of the different tested samples. It can be observed that the kinetics of all the samples are a pretty straight line with different slope, corresponding to the average filtering rate compared for each sample in Figure 12.

Label	1A	2A	3A	4	5	6
Alloy	43500	43500	43500	43500	43500	43500
Comments	Mg0,2 - pure	Mg0,2 - 20% scrap	Mg0,2 - 40% scrap	Mg0,2 - 60% scrap	Mg0,2 - 80% scrap	Mg0,2 - 100% scrap
Final Weight (kg)	1.416	1.432	1.406	1.415	1.403	1.402
Duration (sec)	85	100	109	112	134	140
Filtering rate (g/s)	16.7	14.3	12.9	12.6	10.5	10.0

Table 8: Chemical composition measured on the inspected plate for the different levels of scrap with the AlSi10MnMg0.45 alloy variant

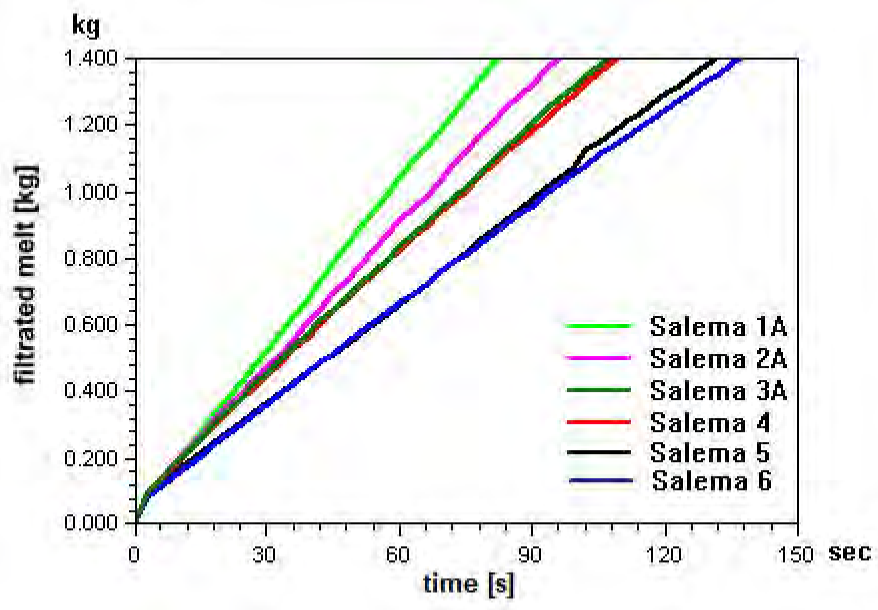

Figure 11. The curves of the filtration kinetics of the tested samples 1-6

The project has received funding from the European Union's Horizon 2020 research and innovation programme under grant agreement No 101003785

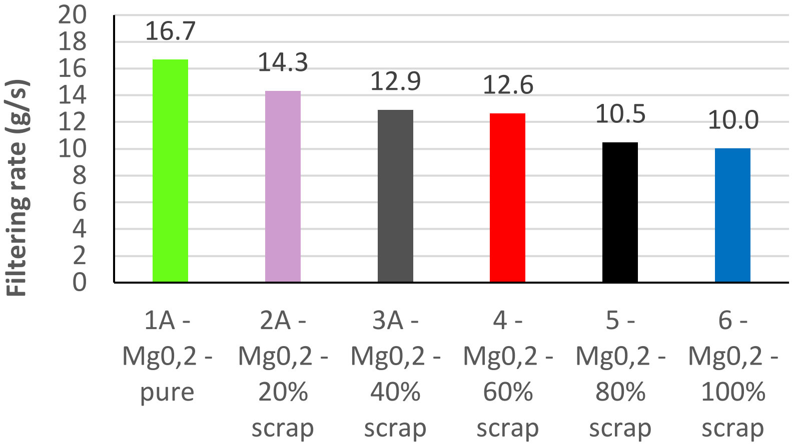

Figure 12. Filtering rate of the tested samples 1-6

In Figure 13 are presented general optical microscope images of the inclusions left in the filter after the Prefil Footprinter® test. It can be observed that the total dimensions of the slurry generated in the filter highly increases with the amount of scrap present in the material filtered.

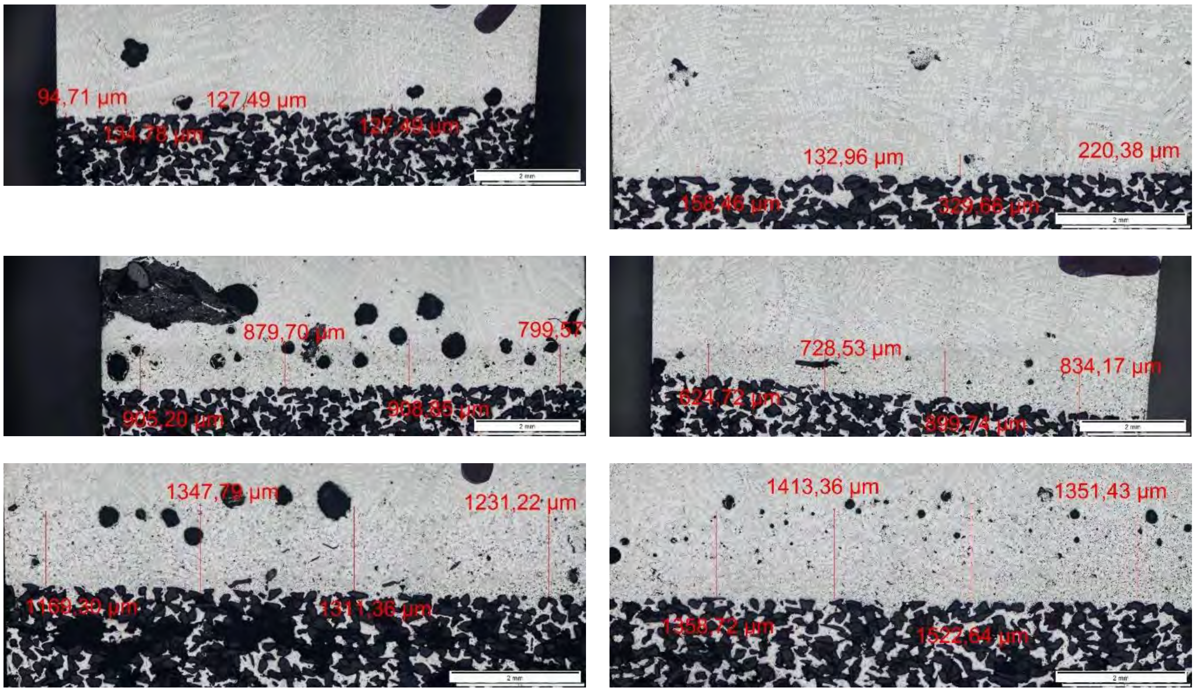

Figure 13. General optical microscope image of samples: 1) top left, 2) top right, 3) centre left, 4) centre right, 5) bottom left and 6) bottom right

In Figure 14 are shown SEM images with the identification of some of particles found in the slurry and in Table 9 and Figure 15 are presented the amount of each kind of particles detected for each of the samples.

The project has received funding from the European Union's Horizon 2020 research and innovation programme under grant agreement No 101003785

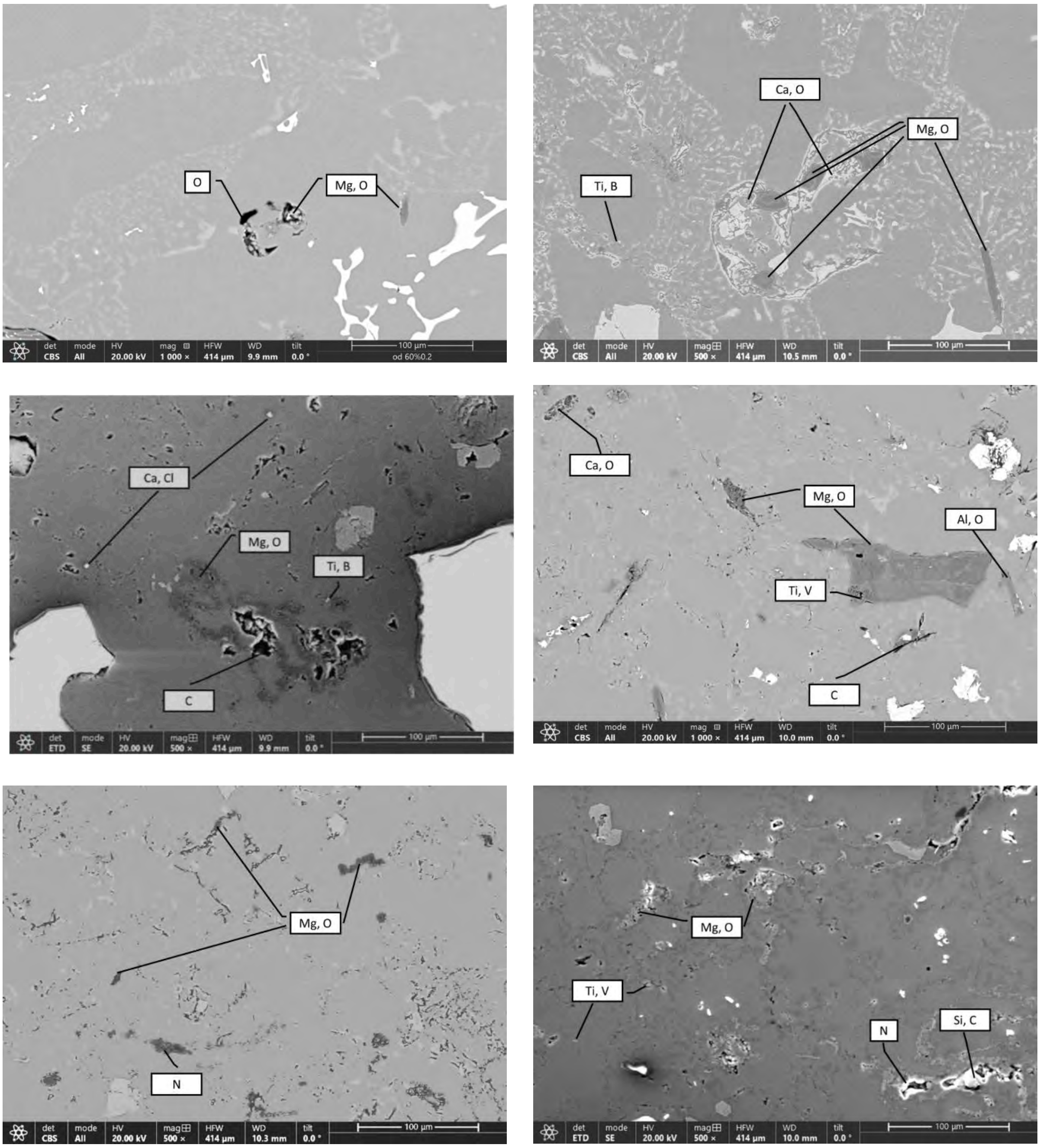

Figure 14. SEM images with particle identification of the different samples: 1) top left, 2) top right, 3) centre left, 4) centre right, 5) bottom left and 6) bottom right

From the results, it can be observed that the quantity of almost every kind of particle retained by the Prefil Footprinter® filter highly increases by using a higher amount of scrap to produce the alloy. This increment is especially clear in the quantity present of magnesium oxides, refractory materials and uncommon inclusions.

The project has received funding from the European Union's Horizon 2020 research and innovation programme under grant agreement No 101003785

Sample number			1A	2A	3A	4	5	6
Inclusion	Chemical symbol	Unit						
Oxide Films	γ-Al_2O_3	#/kg	13	126	998	1225	1197	2313
		Length/ Thickness	short./ thin	short./ thin	short./ thin	short./ thin	med../ thin. med.	med.. long./ thin. med.
Carbides	Al_4C. SiC	mm²/kg	0.0045	0.0135	0.0176	0.0058	0.0170	0.0073
		%	46	34	7	2	4	2
Magnesium Oxides	MgO. $MgAl_2O_4$ – cuboid. $MgAl_2O_4$ - spinel	mm²/kg	0.0000	0.0151	0.1424	0.1752	0.2808	0.3000
		%	0	38	54	71	71	79
Refractory Materials	Spinel-like. CaO. SiO_2. graphite	mm²/kg	0.0029	0.0110	0.0198	0.0296	0.0615	0.0341
		%	29	27	7	12	16	9
Metal treatments	Potential chloride MgCl. NaCl. $CaCl_2$. Fluxing salt	mm²/kg	0.0000	0.0000	0.0000	0.0014	0.0010	0.0004
		%	0	0	0	1	0	0
Uncommon Inclusions	$Ca_3(PO_4)_2$. AlN. FeO/MnO. Si. Fluoride	mm²/kg	0.0024	0.0002	0.0798	0.0290	0.0244	0.0257
		%	24	1	30	12	6	7
Additions	$(Ti.V)B_2$. AlP. TiB_2. TiC	mm²/kg	0.0002	0.0003	0.0042	0.0062	0.0083	0.0115
		%	2	1	2	2	2	3
Total Inclusion Content		mm²/kg	0.0100	0.0401	0.2638	0.2471	0.3930	0.3789
Class			Very Light	Very Light	Moderate	Moderate	Moderate	Moderate

Table 9: Metallographic Analysis Results: Quantification of each inclusion identified for samples 1-6.

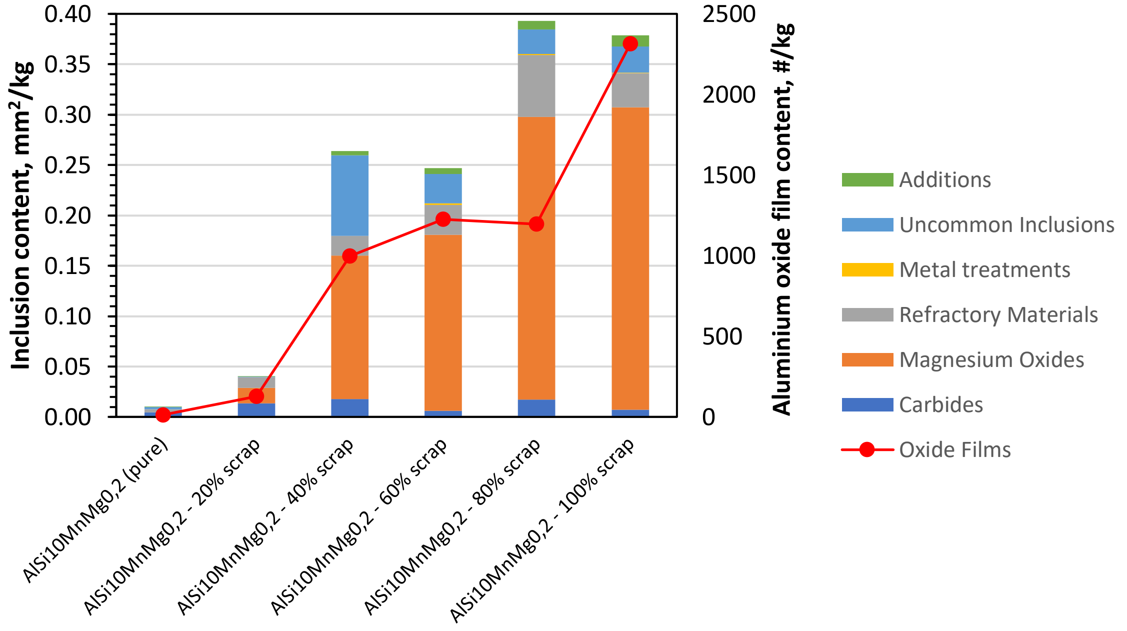

Figure 15. Histogram of Results: Quantification of each inclusion identified for samples 1-6

The project has received funding from the European Union's Horizon 2020 research and innovation programme under grant agreement No 101003785

EN AC 43500 (~0,3 % Mg)

In Table 10 are presented the main features obtained by the Prefil Footprinter® analysis for the AlSi10MnMg alloy with a content of 0.3 % of Mg. Alternatively to the alloy with a 0.2 of Mg content, the filtering rate, duration and final weight remain almost constant and it is independent from the amount of scrap used to produce the alloy. In the details of the filtering kinetics of Figure 16 and the filtering rate of Figure 17.

Label	7	8	9	10	11
Alloy	43500	43500	43500	43500	43500
Comments	Mg0,3 - pure	Mg0,3 - 20% scrap	Mg0,3 - 40% scrap	Mg0,3 - 60% scrap	Mg0,3 - 80% scrap
Final Weight (kg)	1.412	1.416	1.422	1.408	1.413
Duration (sec)	139	136	121	146	146
Filtering rate (g/s)	10.2	10.4	11.8	9.6	9.7

Table 10: Metallographic Analysis Results: Quantification of each inclusion identified for samples 1-6.

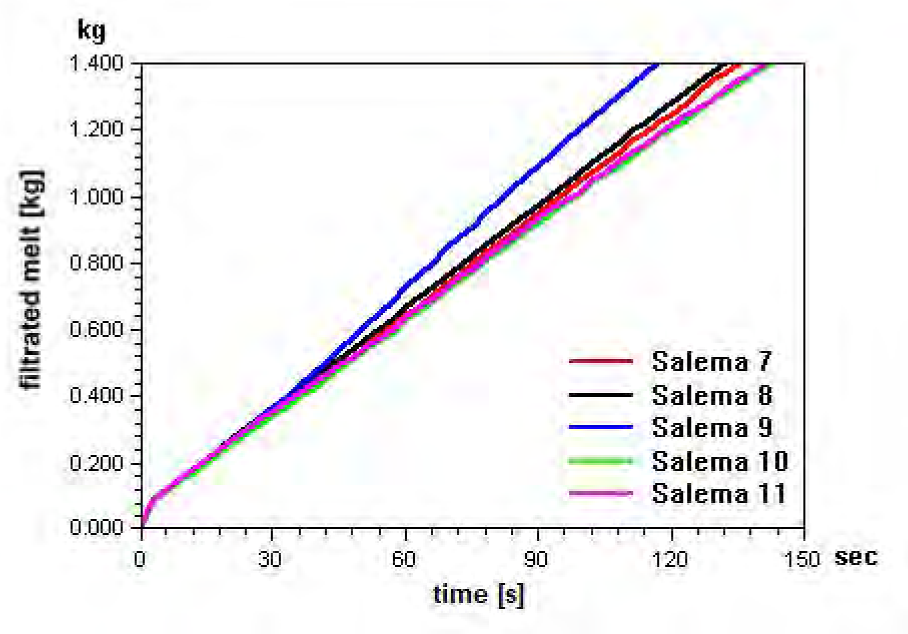

Figure 16. The curves of the filtration kinetics of the tested samples 7-11 43500 alloy

The project has received funding from the European Union's Horizon 2020 research and innovation programme under grant agreement No 101003785

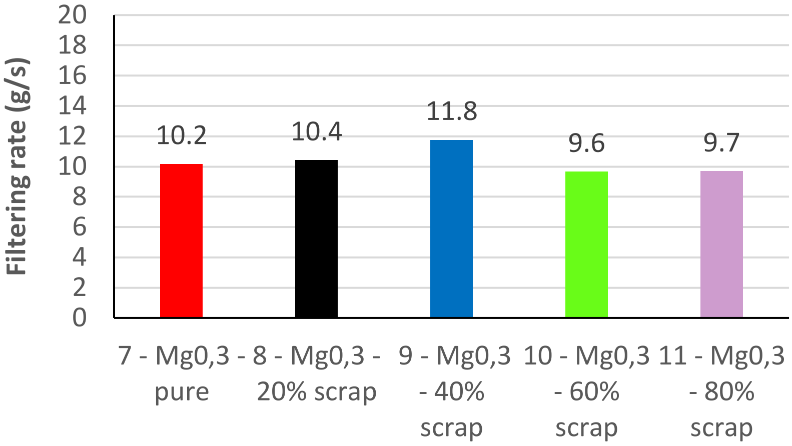

Figure 17. Filtering rate of the tested samples 7-11

In Figure 18 are presented general optical microscope images of the inclusions left in the filter after the Prefil Footprinter® test. It can be observed that the total dimensions of the slurry filtered remains in the size, independently of the scrap ratio used to produce the alloy.

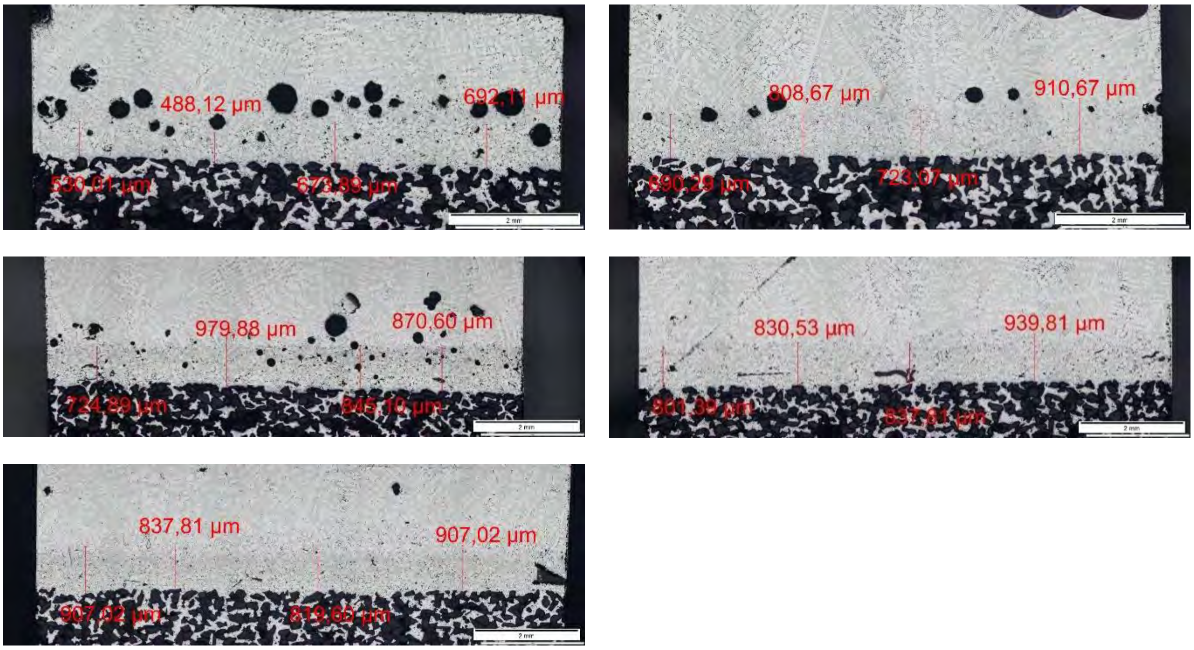

Figure 18. General optical microscope image of samples: 7) top left, 8) top right, 9) centre left, 10) centre right and 11) bottom left

In Figure 19 are shown SEM images with the identification of some of particles found in the slurry and in Table 11 and Figure 20 are presented the amount of each kind of particles detected for each of the samples.

From the analysis of the mud retained by the Prefil Footprinter®, it can be observed that there are a couple of types of inclusions that clearly increase with the amount of scrap used (magnesium oxides and uncommon inclusions), another that decreases (refractory materials) and the others that remain more or less in the same level.

The project has received funding from the European Union's Horizon 2020 research and innovation programme under grant agreement No 101003785

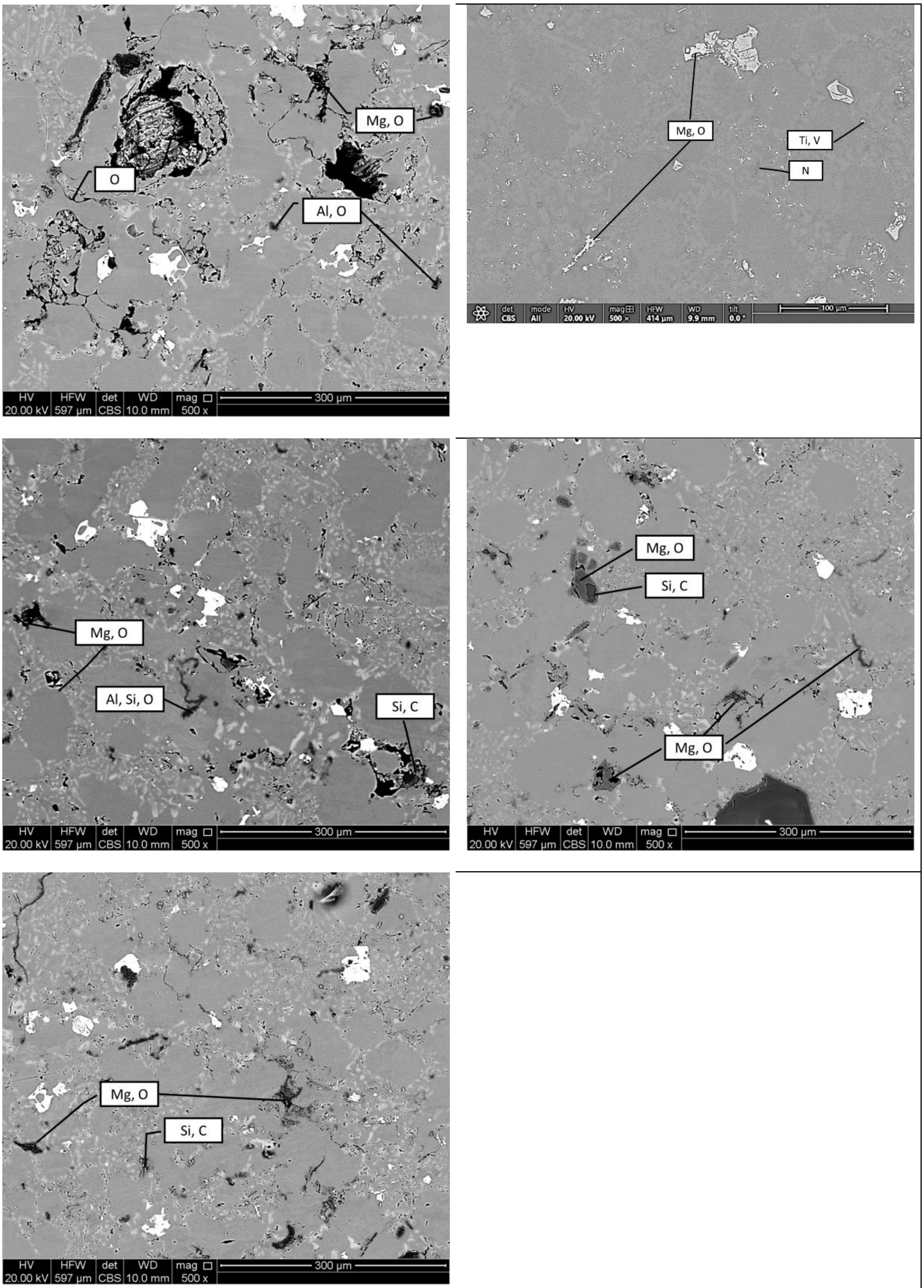

Figure 19. SEM images with particle identification of the different samples: 7) top left, 8) top right, 9) centre left, 10) centre right and 11) bottom left

Sample number			7	8	9	10	11
Inclusion	Chemical symbol	Unit					
Oxide Films	γ-Al_2O_3	#/kg	756	499	857	726	806
		Length/ Thickness	short. med.. long./ thin. med.	med.. long./ thin. med.	med.. long./ thin. med.	med.. long./ thin. med.	med.. long./ thin. med.
Carbides	Al_4C. SiC	mm²/kg	0.0081	0.0034	0.0026	0.0043	0.0095
		%	7	2	2	1	3
Magnesium Oxides	MgO. $MgAl_2O_4$ – cuboid. $MgAl_2O_4$ - spinel	mm²/kg	0.0504	0.0905	0.0539	0.2881	0.2208
		%	41	57	38	88	70
Refractory Materials	Spinel-like. CaO. SiO_2. graphite	mm²/kg	0.0288	0.0261	0.0215	0.0111	0.0097
		%	24	16	15	3	3
Metal treatments	Potential chloride MgCl. NaCl. $CaCl_2$. Fluxing salt	mm²/kg	0.0049	0.0032	0.0045	0.0039	0.0046
		%	4	2	3	1	1
Uncommon Inclusions	$Ca_3(PO_4)_2$. AlN. FeO/MnO. Si. Fluoride	mm²/kg	0.0012	0.0203	0.0253	0.0017	0.0390
		%	1	13	18	1	12
Additions	$(Ti.V)B_2$. AlP. TiB_2. TiC	mm²/kg	0.0285	0.0155	0.0334	0.0175	0.0337
		%	23	10	24	5	11
Total Inclusion Content		mm²/kg	0.1220	0.1591	0.1412	0.3266	0.3174
Class			Moderate	Moderate	Moderate	Moderate	Moderate

Table 11: Metallographic Analysis Results: Quantification of each inclusion identified for samples 7-11

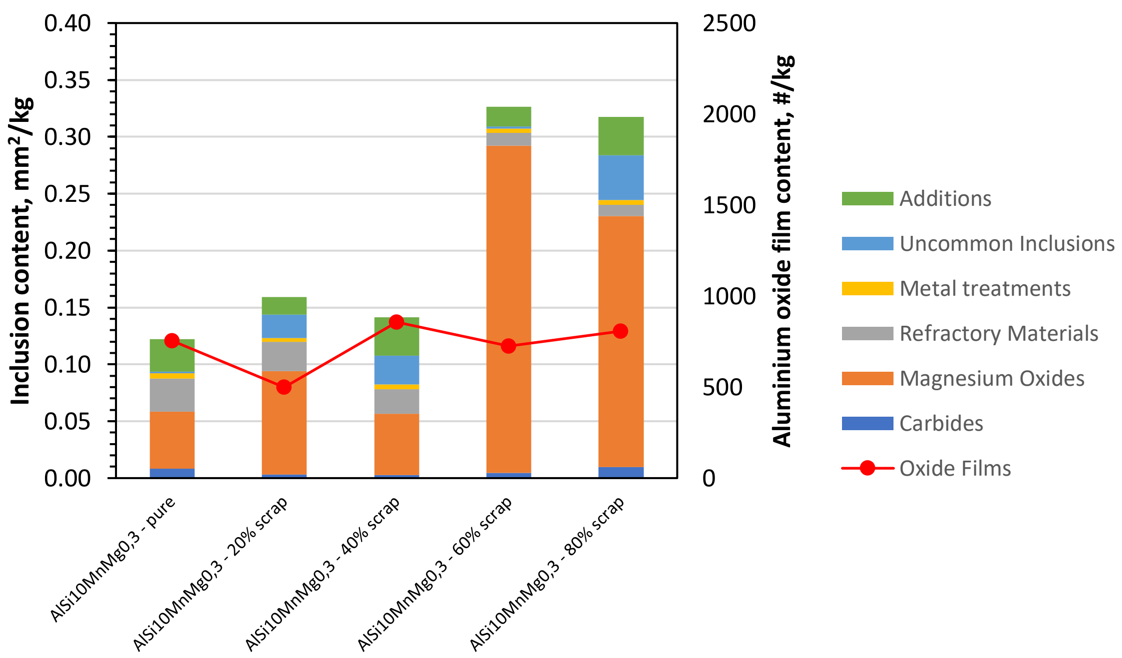

Figure 20. Histogram of Results: Quantification of each inclusion identified for samples 7-11

The project has received funding from the European Union's Horizon 2020 research and innovation programme under grant agreement No 101003785

EN AC 43500 (~0,45 % Mg)

In Table 12 are presented the main features obtained by the Prefil Footprinter® analysis for the AlSi10MnMg alloy with a content of 0.45 % of Mg. It is observed that the duration increases, and the filtering rate slightly decreases with the amount of scrap used to produce the alloy, but at a rate much slower than the observed for the alloy with a 0.2 of Mg content. The details of the filtering kinetics of Figure 21 and the filtering rate of Figure 22 show the same trend.

Label	12	13	14
Alloy	43500	43500	43500
Comments	Mg0,45 - pure	Mg0,45 - 20% scrap	Mg0,45 - 40% scrap
Final Weight (kg)	1.411	1.411	1.392
Duration (sec)	124	134	150
Filtering rate (g/s)	11.4	10.5	9.3

Table 12: Measurement results with the Prefil device for samples 12-14

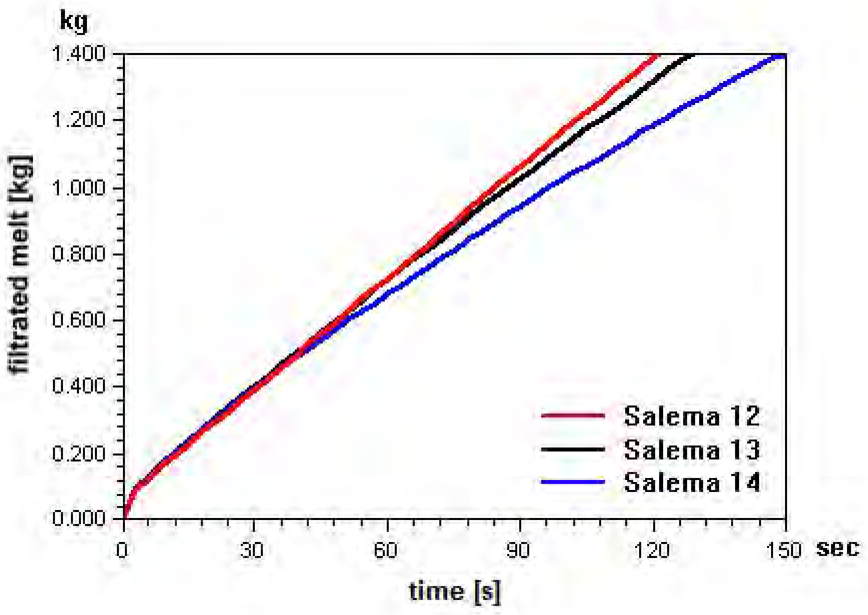

Figure 21. The curves of the filtration kinetics of the tested samples 12-14

The project has received funding from the European Union's Horizon 2020 research and innovation programme under grant agreement No 101003785

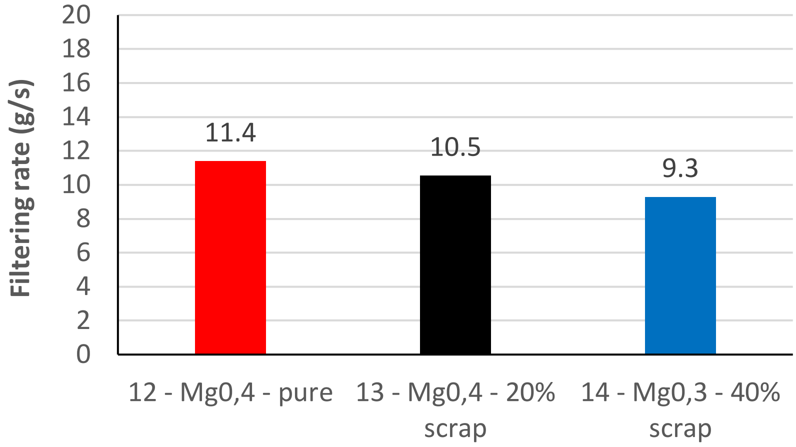

Figure 22. Filtering rate of the tested samples 12-14

In Figure 23 are presented general optical microscope images of the inclusions left in the filter after the Prefil Footprinter® test. It can be observed that the total dimensions of the slurry slightly increase with the amount of scrap used to produce the alloy.

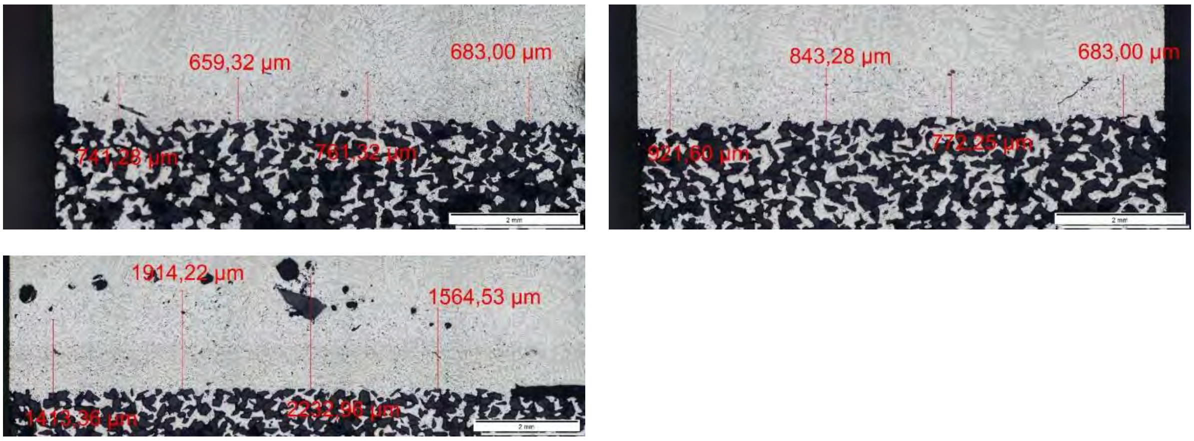

Figure 23. General optical microscope image of samples: 12) top left, 13) top right and 14) bottom left

In Figure 24 are shown SEM images with the identification of some of particles found in the slurry and in Table 13 and Figure 25 are presented the amount of each kind of particles detected for each of the samples.

The project has received funding from the European Union's Horizon 2020 research and innovation programme under grant agreement No 101003785

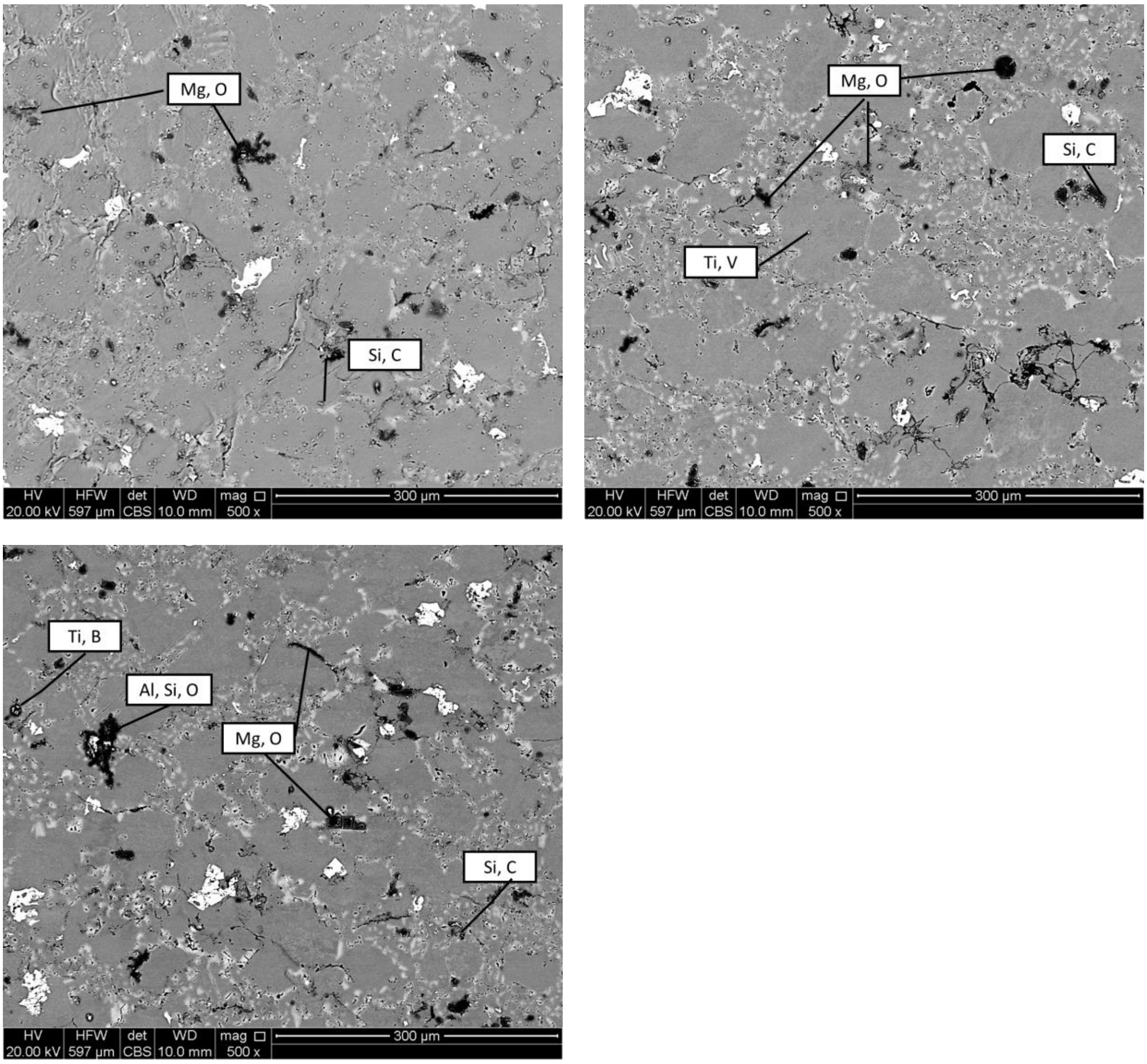

Figure 24. SEM images with particle identification of the different samples: 12) top left, 13) top right and 14) bottom left

In this case the results obtained from the analysis of the particles retained in the filter by the Prefil Footprinter® from Table 13 do not show any relevant trend. The values for the different type of particles remain more or less in the same level, without showing a clear trend.

The project has received funding from the European Union's Horizon 2020 research and innovation programme under grant agreement No 101003785

Sample number			12	13	14
Inclusion	Chemical symbol	Unit			
Oxide Films	γ-Al_2O_3	#/kg	454	726	1532
		Length/ Thickness	short. med.. long./ thin. med.	short. med.. long./ thin. med.	short. med.. long./ thin. med.
Carbides	Al_4C. SiC	mm²/kg	0.0399	0.0186	0.0086
		%	18	11	3
Magnesium Oxides	MgO. $MgAl_2O_4$– cuboid. $MgAl_2O_4$ - spinel	mm²/kg	0.1252	0.1023	0.1563
		%	57	63	59
Refractory Materials	Spinel-like. CaO. SiO_2. graphite	mm²/kg	0.0216	0.0181	0.0443
		%	10	11	17
Metal treatments	Potential chloride MgCl. NaCl. $CaCl_2$. Fluxing salt	mm²/kg			
		%			
Uncommon Inclusions	$Ca_3(PO_4)_2$. AlN. FeO/MnO. Si. Fluoride	mm²/kg	0.0087	0.0036	0.0078
		%	4	2	3
Additions	(Ti.V)B_2. AlP. TiB_2. TiC	mm²/kg	0.0229	0.0193	0.0488
		%	10	12	18
Total Inclusion Content		mm²/kg	0.1619	0.2182	0.2658
Class			Moderate	Moderate	Moderate

Table 13: Metallographic Analysis Results: Quantification of each inclusion identified for samples 12-14

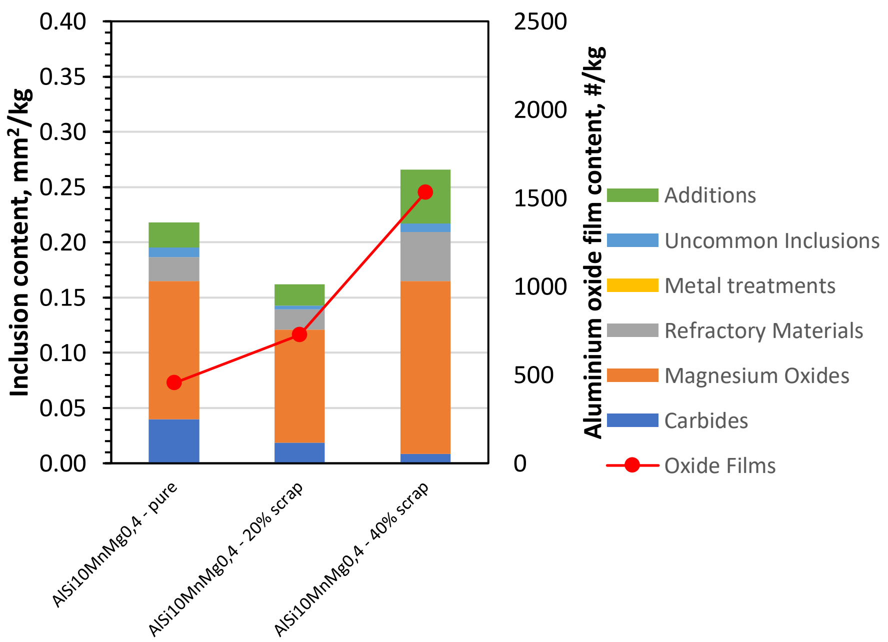

Figure 25. Histogram of Results: Quantification of each inclusion identified for samples 12-14

The project has received funding from the European Union's Horizon 2020 research and innovation programme under grant agreement No 101003785

2.2.4. Microstructure observed

In Figure 26, Figure 28 and Figure 30 are presented the low magnification optical microscope images obtained for the different scrap ratios. The general microstructure of all the samples is quite similar, showing Al dendrites of similar sizes, similar proportion of Al-Si eutectic and other intermetallic phases.

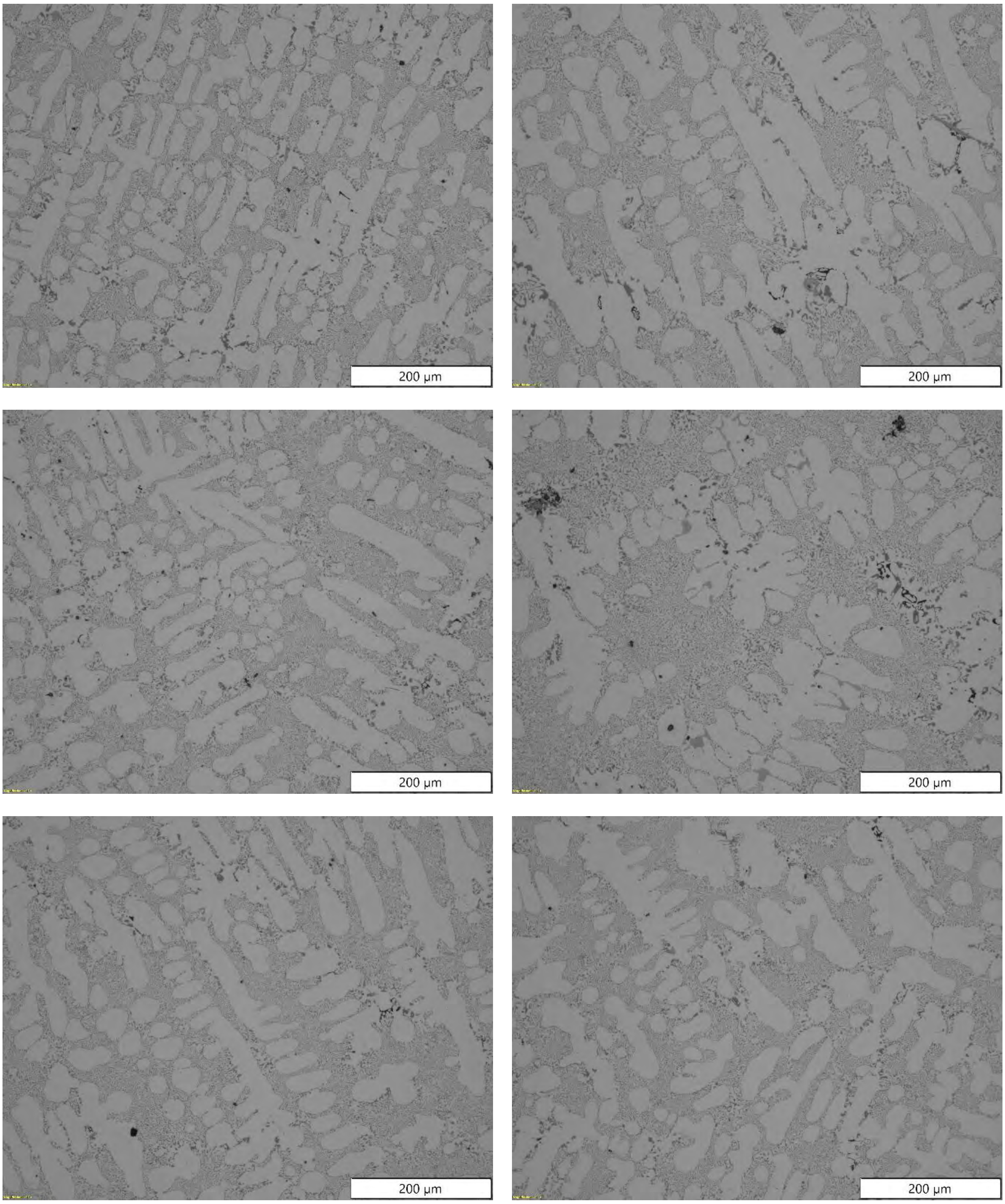

Figure 26. Low magnification microstructure of the alloy variant with 0.3% of Mg, produced with different scrap content: top left 0%, top right 20%, medium left 40%, medium right 60%, bottom left 80% and bottom right 100%.

The project has received funding from the European Union's Horizon 2020 research and innovation programme under grant agreement No 101003785

In Figure 27, Figure 29 and Figure 31 are presented the high magnification images obtained by optical microscope of the samples produced for the different scrap ratios. The general microstructure of all the samples is quite similar, showing a similar amount and distribution of intermetallic particles.

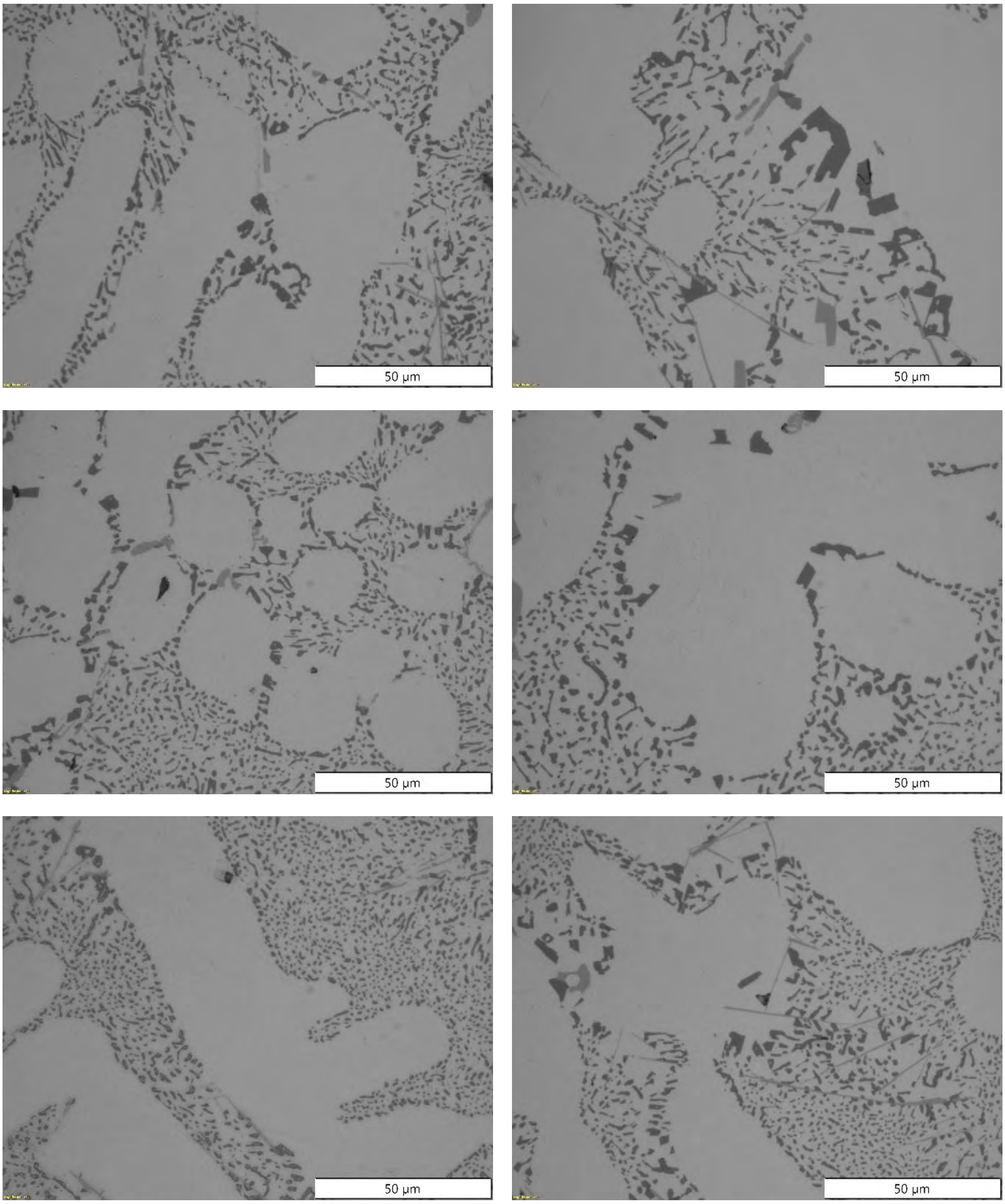

Figure 27. High magnification microstructure of the alloy variant with 0.3% of Mg, produced with different scrap content: top left 0%, top right 20%, medium left 40%, medium right 60%, bottom left 80% and bottom right 100%.

The project has received funding from the European Union’s Horizon 2020 research and innovation programme under grant agreement No 101003785

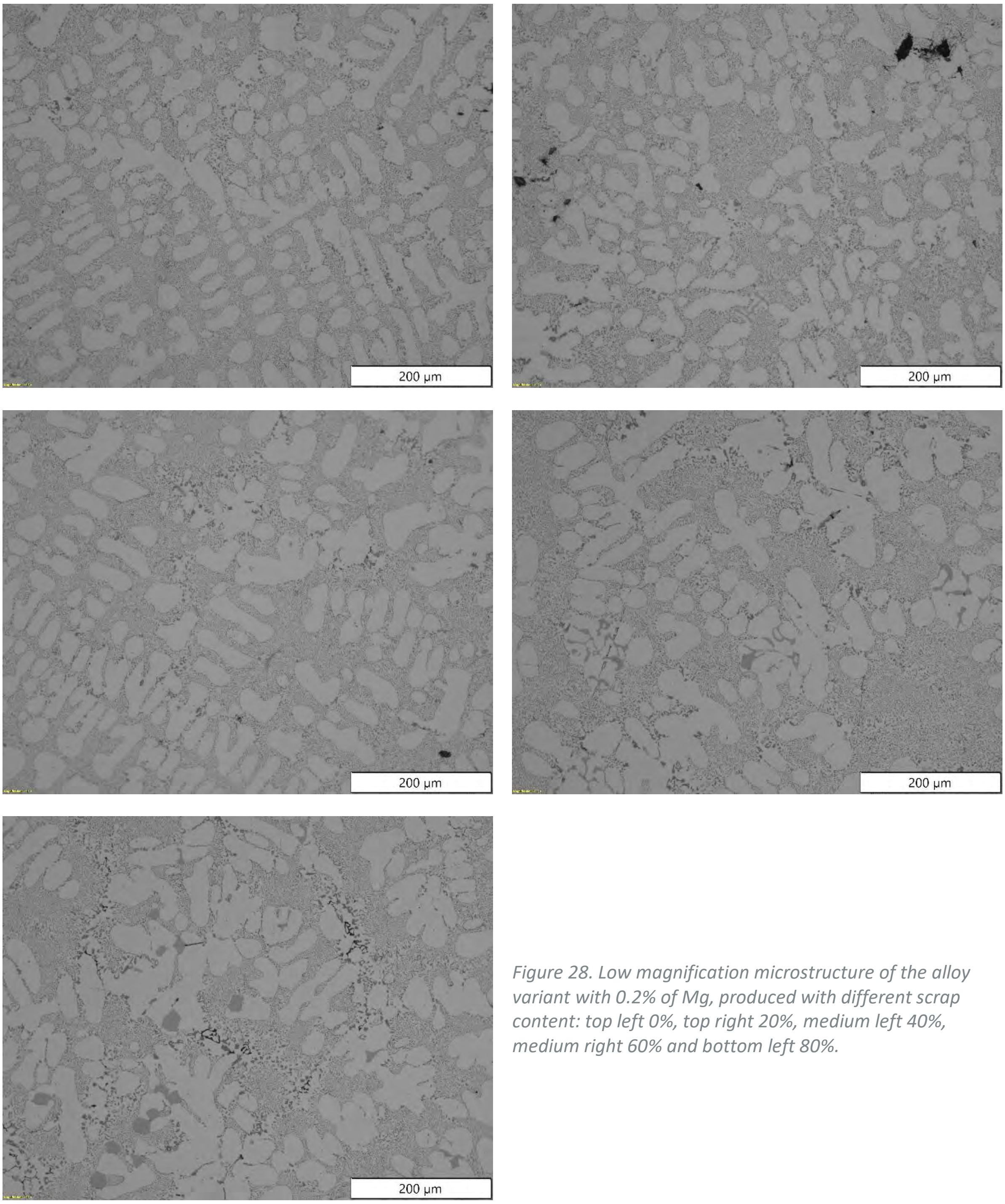

Figure 28. Low magnification microstructure of the alloy variant with 0.2% of Mg, produced with different scrap content: top left 0%, top right 20%, medium left 40%, medium right 60% and bottom left 80%.

The project has received funding from the European Union's Horizon 2020 research and innovation programme under grant agreement No 101003785

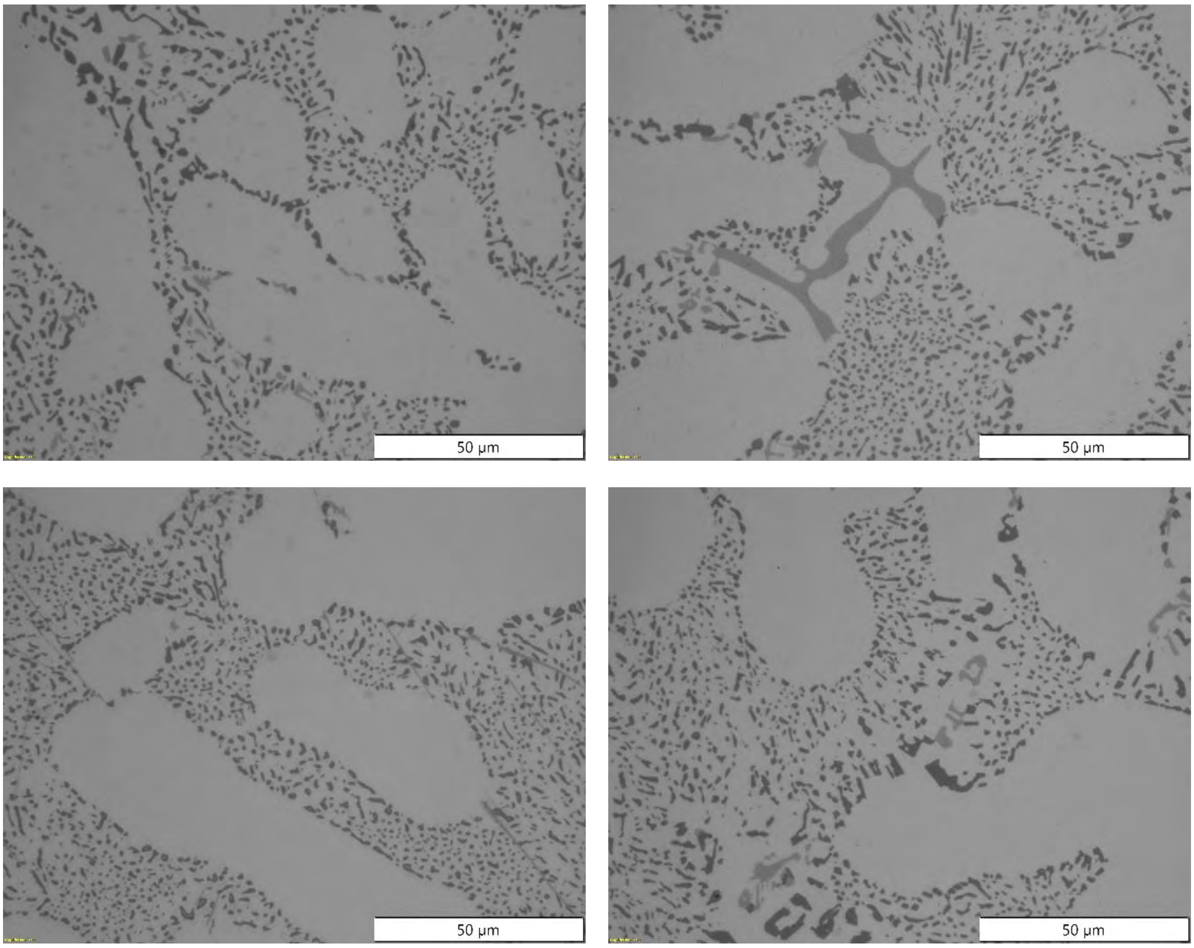

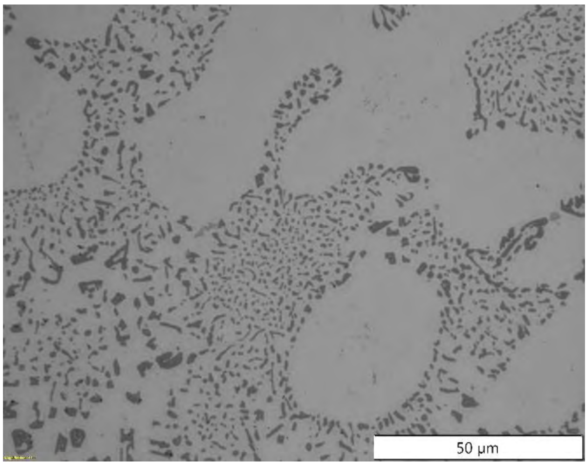

Figure 29. High magnification microstructure of the alloy variant with 0.2% of Mg, produced with different scrap content: top left 0%, top right 20%, medium left 40%, medium right 60% and bottom left 80%.

The project has received funding from the European Union’s Horizon 2020 research and innovation programme under grant agreement No 101003785

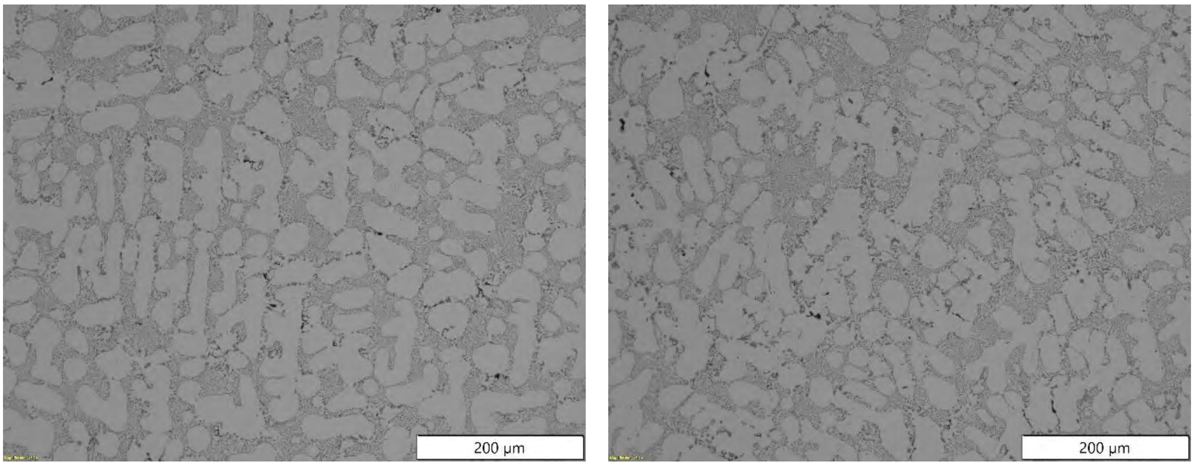

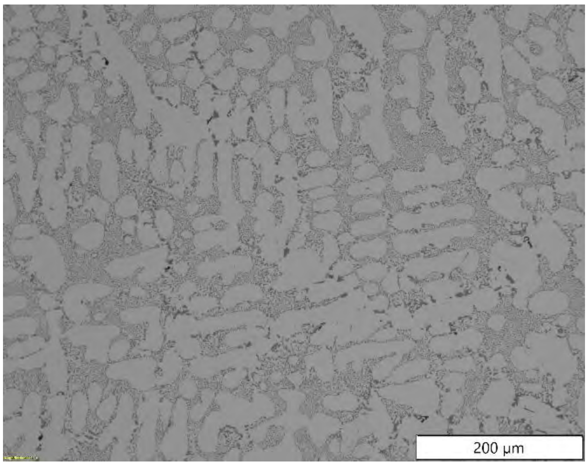

Figure 30. Low magnification microstructure of the alloy variant with 0.45% of Mg, produced with different scrap content: top left 0%, top right 20% and medium left 40%.

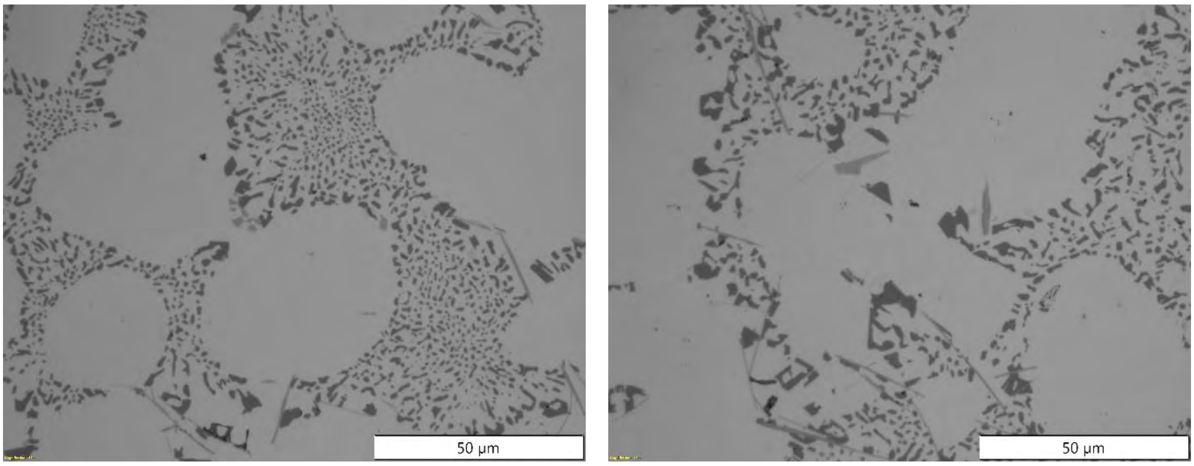

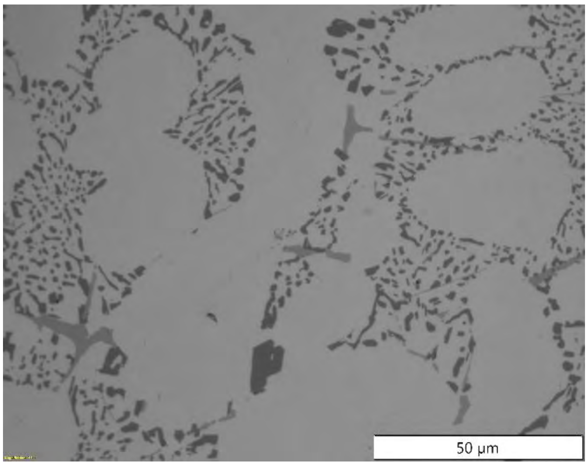

Figure 31. High magnification microstructure of the alloy variant with 0.45% of Mg, produced with different scrap content: top left 0%, top right 20% and medium left 40%.

2.2.5. Mechanical properties

In Table 14 are presented the main results obtained with the tensile tests conducted for the different materials. It can be observed that the mechanical properties remain in the same level independently of the amount of scrap material used. On the other hand, it can be observed that the mechanical resistance slightly increases and elongation slightly decreases with Mg content.

Material	σ_{YS} [Mpa]	σ_{UTS} [Mpa]	A_{25} [%]
AlSi10MnMg0.2	99	167	5.5
AlSi10MnMg0.2 + 20% scrap	93	158	4.9
AlSi10MnMg0.2 + 40% scrap	98	170	6.9
AlSi10MnMg0.2 + 60% scrap	100	173	5.9
AlSi10MnMg0.2 + 80% scrap	82	164	7.3
100 % AlSi10MnMg scrap	98	180	5.7
AlSi10MnMg0.3	111	184	3.8
AlSi10MnMg0.3 + 20% scrap	104	187	5.7
AlSi10MnMg0.3 + 40% scrap	100	178	4.7
AlSi10MnMg0.3 + 60% scrap	89	159	4.9
AlSi10MnMg0.3 + 80% scrap	97	179	6.3
AlSi10MnMg0.45	113	176	3.4
AlSi10MnMg0.45 + 20% scrap	102	181	4.8
AlSi10MnMg0.45 + 40% scrap	105	179	5.1

Table 14. Mechanical properties obtained with the tensile tests conducted for the different Mg concentrations and scrap ratio

2.3. Comments and remarks

The results obtained for the HPDC alloys show that the introduction of scrap has a negative impact on the number of inclusions present in the melt, mainly due to the presence of oxides and other impurities, that also reduces the melt flowability.

The project has received funding from the European Union’s Horizon 2020 research and innovation programme under grant agreement No 101003785

This is especially remarkable for the alloy with a lower Mg content, in which the quantity of particles and flowability seems to be more easily affected by the scrap content.
Nevertheless, seems that most of the new inclusions related with the use of scrap are oxides, that can be easily removed from the melt with rotary degassing, use of fluxes or any other standard melt treatment.

3. Laboratory trials with extrusion alloys

3.1. Experimental methodology

3.1.1. Alloys and material format supplied by ASAS

The material used as reference for the initial development of SALEMA extrusion alloys where billets produced by ASAS, in the format that they provide them to their customers, of 6063 alloy (Figure 32). ASAS produced and delivered billets of 6" (152 mm) of diameter and about 50 mm thick. The quality certificate provided by ASAS for those billets is presented in ANNEX 2.

Figure 32. Image of the ingots supplied by ASAS for WP1 trials related with extrusion alloys

The chemical composition of a piece of a billet of each was also measured by Eurecat, in order to have a second measurement with the same equipment and procedure used for measuring the casting samples. In Table 15 are presented the chemical analysis obtained by arc/spark optical emission spectroscopy with Eurecat SPECTROMAXx spectrometer. The equipment and experimental procedure were already presented in detail in Deliverable 1.2. The same equipment and procedure were also used to measure the chemical compositions of the cast parts and the rest of compositions reported in this document.

n=5	%Si	% Fe	%Cu	%Mn	%Mg	%Cr	%Ni	%Sn
6063 alloy	0.58	0.20	<0.03	0.03	0.48	<0.03	<0.03	<0.03

Table 15. Chemical composition measured at Eurecat for the 3 samples taken from each reference alloys lots provided by Raffmetal

3.1.2. Scrap used to mix with reference material

Eurecat had to acquire a large amount of scrap of 6063 aluminium extruded profile for a different project. The scrap was supplied in a large plastic container of 1m^3 of volume (Figure 33). With a general sight it was clear that all the scrap supplied was exclusively aluminium extruded profile, but of different shapes, thicknesses, and some of them were painted or had a surface treatment. A selection of 10 representative pieces were taken from the container, in order to have a precise chemical analysis of them.

Figure 33: General overview of the 6063 extruded profile acquired from a local aluminium recycling company (left) and image of the 10 parts selected for a Spark Plasma chemical analysis (right)

The results of the chemical analysis of the 10 selected parts are presented in Table 16. It can be observed that the scrap is quite homogeneous and of similar composition. The compositions of all 10 pieces correspond to a 6063 alloy, just in some of them the Mg content is a little lower than the minimum content permitted for the alloy and should be considered as a 6060 alloy.

n=5	%Si	% Fe	%Cu	%Mn	%Mg	%Zn	%Ni	%Cr	%Pb	%Sn	%Ti
Spec 1	0.42	0.23	<0.01	0.05	0.36	<0.01	<0,01	<0,01	<0,01	<0,01	0.01
Spec 2	0.42	0.26	0.03	0.06	0.43	0.04	<0,01	<0,01	<0,01	<0,01	0.02
Spec 3	0.42	0.21	<0.01	0.03	0.38	<0.01	<0.01	<0.01	<0.01	<0.01	0.01
Spec 4	0.43	0.22	<0.01	0.03	0.40	<0.01	<0,01	<0,01	<0,01	<0,01	0.01
Spec 5	0.41	0.24	0.02	0.04	0.45	0.04	<0,01	<0,01	<0,01	<0,01	0.02
Spec 6	0.41	0.23	0.02	0.03	0.38	<0.01	<0.01	<0.01	<0.01	<0.01	0.01
Spec 7	0.49	0.23	0.01	0.03	0.48	0.01	<0.01	<0.01	<0.01	<0.01	0.02
Spec 8	0.53	0.19	0.02	0.08	0.44	<0.01	<0,01	<0,01	<0,01	<0,01	0.02
Spec 9	0.56	0.23	0.02	0.06	0.44	0.01	<0,01	<0,01	<0,01	<0,01	0.01
Spec 10	0.42	0.21	0.01	0.03	0.57	0.01	<0.01	<0.01	<0.01	<0.01	0.02
6063	**0.2-0.6**	**0.35**	**0.1**	**0.1**	**0.45-0.9**	**0.1**	**0.05**	**0.1**	**0.05**	**0.05**	**0.1**

Table 16: Chemical composition measured by spark OES with SPECTROMAXx equipment on the 3 fragments selected from the 6xxx extruded profile supplied by a local aluminium recycling company

3.2. Results obtained from the produced samples

3.2.1. Chemical composition of the different batches

Casting samples were produced for 6063 alloys with selected scrap in different percentages, in steps of 20 %, from 0 % to 100 % scrap following the methodology described in section 2.1 for HPDC. The chemical composition of the different samples extracted were measured by Optical Emission Spectrometry and are presented in Table 17.

The project has received funding from the European Union's Horizon 2020 research and innovation programme under grant agreement No 101003785

Chemical composition was relatively stable, with only Silicon content dropping as scrap content was increased- this can be easily solved by introducing small amounts of silicon during recycling.

n=5	%Si	% Fe	%Cu	%Mn	%Mg	%Cr	%Ni	%Zn	%Ti
6063	0.8	0.2	0.02	0.05	0.48	<0.03	<0,03	<0,03	<0,03
Mg0.3-20%scrap	0.72	0.21	0.02	0.05	0.47	<0.03	<0,03	<0,03	<0,03
Mg0.3-40%scrap	0.62	0.21	0.02	0.05	0.47	<0.03	<0,03	<0,03	<0,03
Mg0.3-60%scrap	0.51	0.23	0.01	0.05	0.45	<0.03	<0,03	<0,03	<0,03
Mg0.3-80%scrap	0.51	0.23	0.02	0.06	0.45	<0.03	<0,03	<0,03	<0,03
100 % scrap	0.5	0.23	0.02	0.06	0.43	<0.03	<0,03	<0,03	<0,03
EN AB-43500	9-11.5	<0.20	<0.03	0.4-0.8	0.15-0.6	<0.03	<0,03	<0,03	<0,03

Table 17: Chemical composition measured on the inspected plate for the different levels of scrap with the AlSi10MnMg0.3 alloy variant

In the results reported it is observed that the highest level of impurities belongs to the samples cast with the pure alloy. The level of Fe and Cu are higher than the actual upper limit of the standard for EN AB-43500 alloy. The concentration of those impurities in the samples decreased when scrap was added.

Both elements, have also a higher concentration than the level measured in the specimens extracted from the original ingots (Table 1), which suggest that the higher level of impurities was due to an external contamination. Considering that the 3 first measures correspond to the first batch produced with AlSi10MnMg alloy, it is likely that the reason of such contamination was the presence of rests of a different alloy in the furnace.

3.2.2. Inclusion analysis with Prefil Footprinter®

The presence of inclusions was analysed using the Prefil Footprinter, in a manner analogous to the study presented in section 2.2.3 for HPDC alloy; Table 18 offers an outlook on the performed experiments.

The amount of scrap did not significantly affect the filtering kinetics for the 6063 extrusion alloy. Results, summarized Figure 34 and Figure 35 show no clear trend in modification of the filtering rates, hinting that the use of scrap would not significantly impact the alloy in terms of inclusions severe enough to affect melt flow.

Label	15B	16B	17	18	19A	20A
Alloy	6063	6063	6063	6063	6063	6063
Comments	6063 - pure	6063 - 20% scrap	6063 - 40% scrap	6063 - 60% scrap	6063 - 80 % scrap	6063 - 100 % scrap
Final Weight (kg)	0.687	0.632	0.770	0.649	0.747	0.749
Duration (sec)	150	150	150	150	150	150
Filtering rate (g/s)	4.6	4.2	5.1	4.3	5.0	5.0

Table 18: Measurement results with the Prefil device for samples 15-20

The project has received funding from the European Union's Horizon 2020 research and innovation programme under grant agreement No 101003785

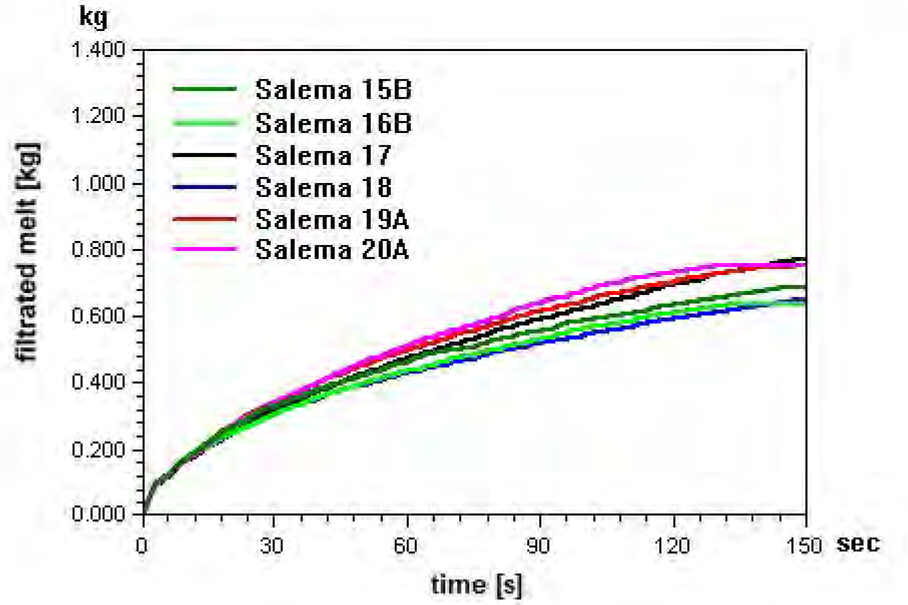

Figure 34. The curves of the filtration kinetics of the tested samples 15-20 6063 alloy

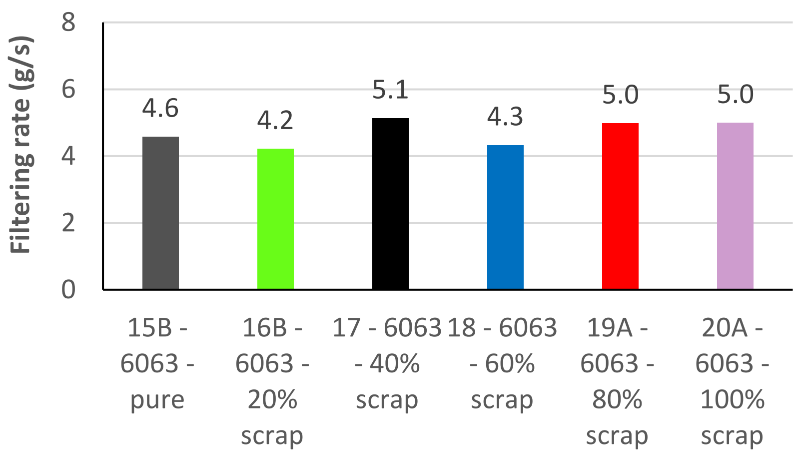

Figure 35. Filtering rate of the tested samples 15-20

These observations match the leftover slurry, shown in overview in Figure 36 and with detailed analysis offered in Figure 37 (SEM imaging of inclusions), Table 19 (quantitative data) and a summary histogram presented in Figure 38.

The presence of inclusions is overall unaffected in both quantity and chemical composition, to the extreme that pure alloy and 100% scrap samples are mostly equivalent in these terms. In fact, the sample showing the best quality and cleanliness is Sample 19, corresponding to 80 % scrap- on the opposite case, sample 18 (60% scrap) showed significantly high amount of inclusions, mainly magnesium oxides. Due to the test procedure, where scrap was sequentially introduced in the furnace

The project has received funding from the European Union's Horizon 2020 research and innovation programme under grant agreement No 101003785

as the different samples were extracted (see description in section 2.1), this suggests that part of the differences observed may be related to chance and variability or even mould contamination for the 60% scrap sample, rather than a trend of alloy degradation.

The exception of this is the presence of carbides, that decreases steadily through the processing steps. This points that carbides were present in the original pure 6063 melt, and carbide content has been diluted by the addition of scrap.

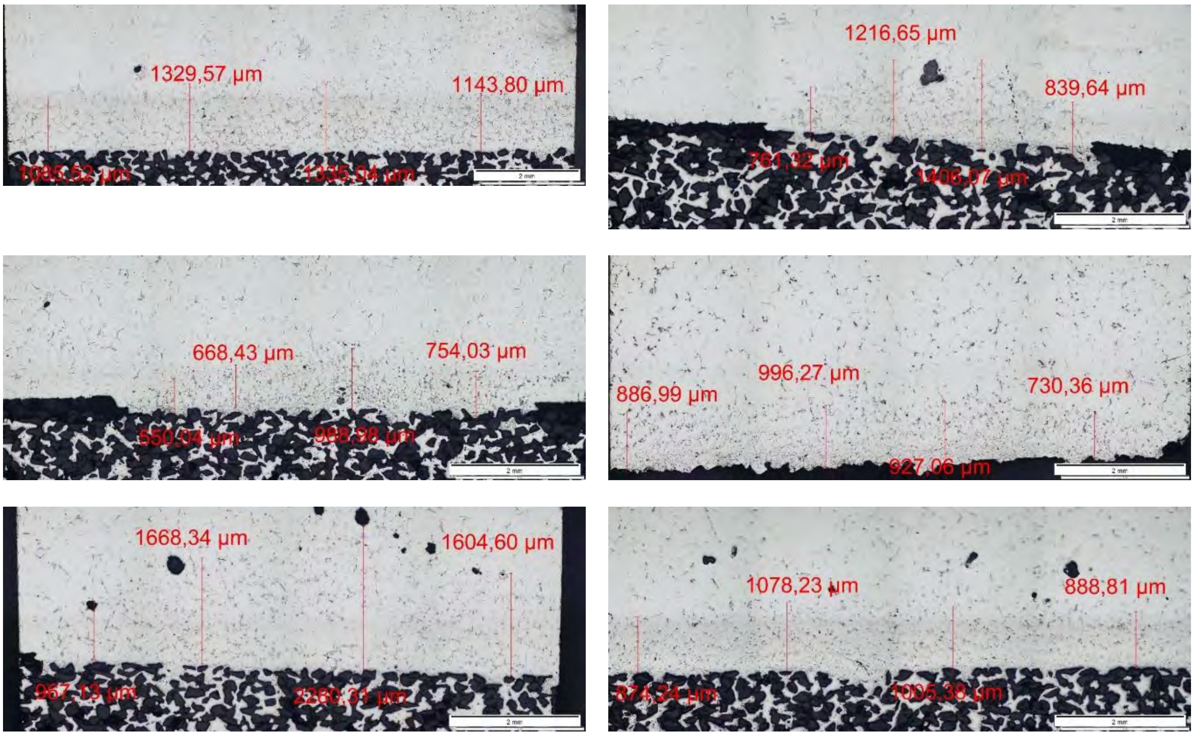

Figure 36. General optical microscope image of samples: 15) top left, 16) top right, 17) centre left, 18) centre right, 19) bottom left and 20) bottom right

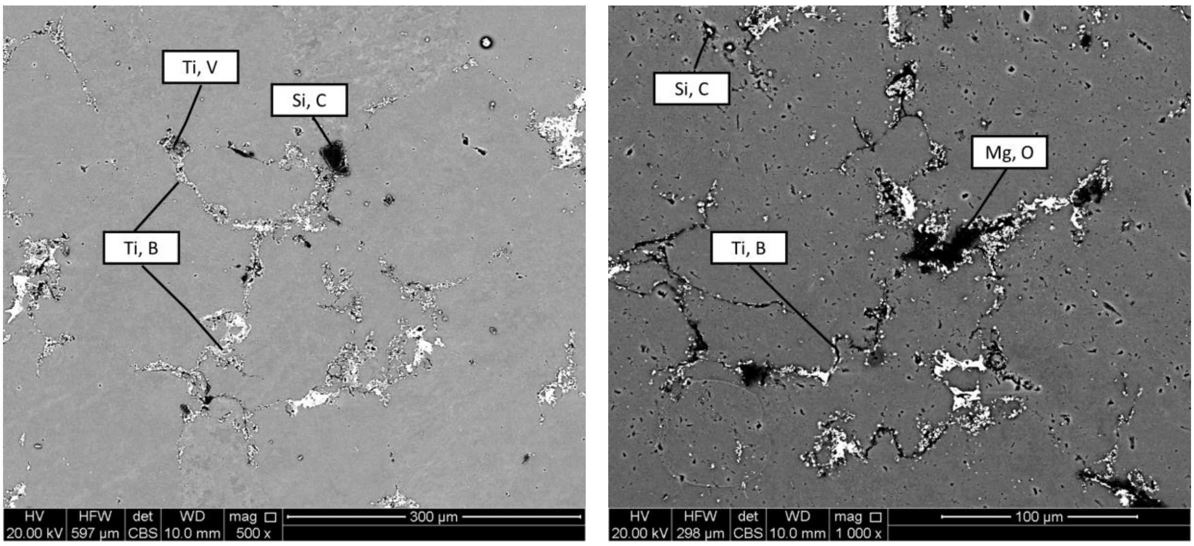

The project has received funding from the European Union's Horizon 2020 research and innovation programme under grant agreement No 101003785

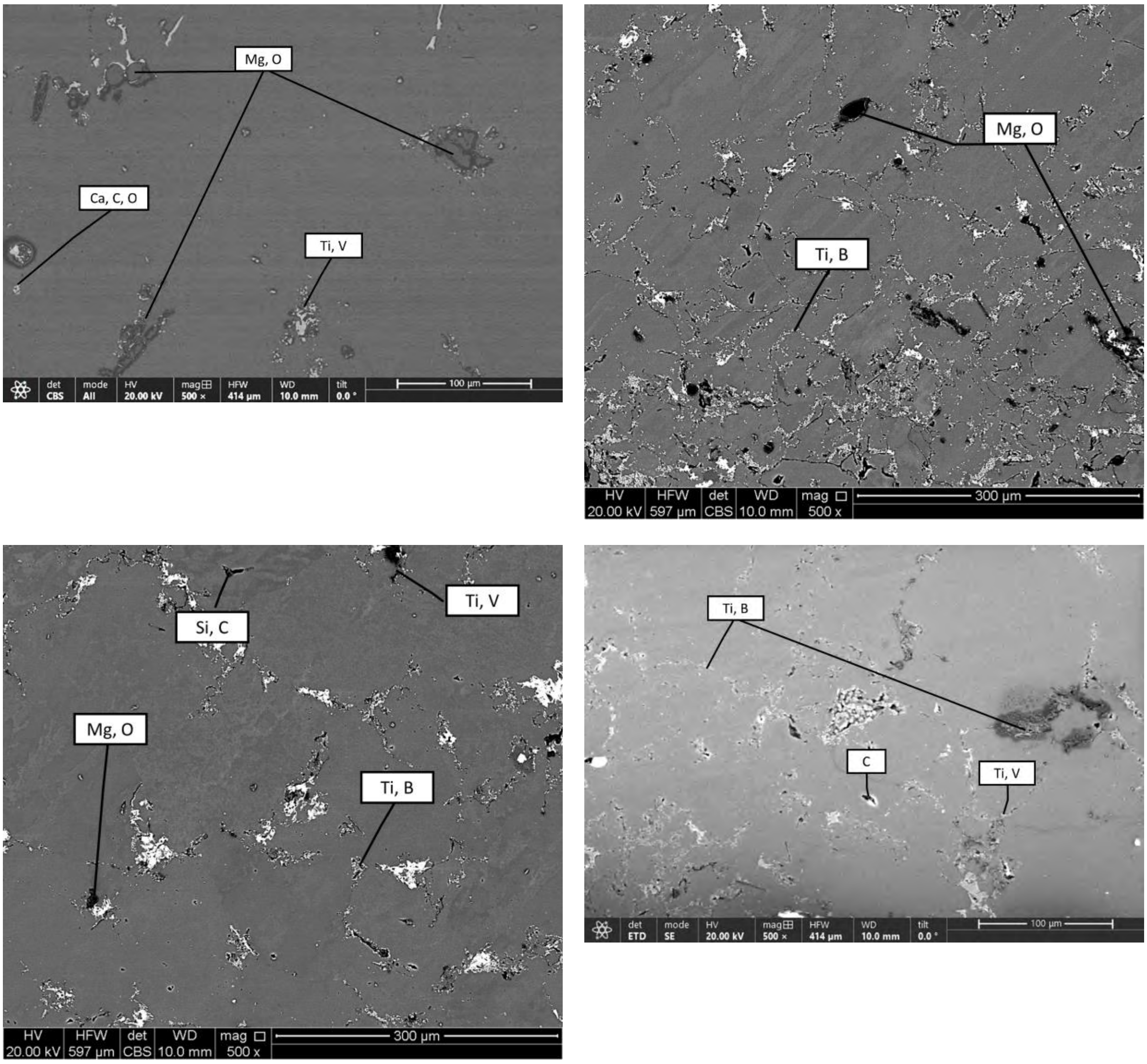

Figure 37. SEM images with particle identification of the different samples: 15) top left, 16) top right, 17) centre left, 18) centre right, 19) bottom left and 20) bottom right

Sample number			15B	16B	17	18	19A	20A
Inclusion	Chemical symbol	Unit						
Oxide Films	γ-Al_2O_3	#/kg	1027	1898	1649	4240	1228	1696
		Length/ Thickness	med.. long./ thin. med.	med.. long./ thin. med.	med.. long./ thin. med.	med.. long./ thin. med.	med.. long./ thin. med.	med.. long./ thin. med.
Carbides	Al_4C. SiC	mm^2/kg	0.0950	0.0261	0.0127	0.0069	0.0141	0.0181
		%	18	6	3	1	7	4
Magnesium Oxides	MgO. $MgAl_2O_4$ – cuboid. $MgAl_2O_4$ - spinel	mm^2/kg	0.0215	0.0678	0.0203	0.1666	0.0061	0.0072
		%	4	16	5	19	3	1
		mm^2/kg	0.0207	0.0057	0.0075	0.0147	0.0022	0.0068

The project has received funding from the European Union's Horizon 2020 research and innovation programme under grant agreement No 101003785

Refractory Materials	Spinel-like. CaO. SiO_2. graphite	%	4	1	2	2	1	1
Metal treatments	Potential chloride MgCl. NaCl. $CaCl_2$. Fluxing salt	mm²/kg						
		%						
Uncommon Inclusions	$Ca_3(PO_4)_2$. AlN. FeO/MnO. Si. Fluoride	mm²/kg	0.0032	0.0152	0.0425	0.0335	0.0126	0.0114
		%	1	4	10	4	6	2
Additions	$(Ti.V)B_2$. AlP. TiB_2. TiC	mm²/kg	0.3930	0.3105	0.3234	0.6390	0.1740	0.4486
		%	74	73	80	74	83	91
Total Inclusion Content		mm²/kg	0.5333	0.4253	0.4064	0.8607	0.2090	0.4922
Class			Heavy	Heavy	Heavy	Heavy	Moderate	Heavy

Table 19: Metallographic Analysis Results: Quantification of each inclusion identified for samples 15-20

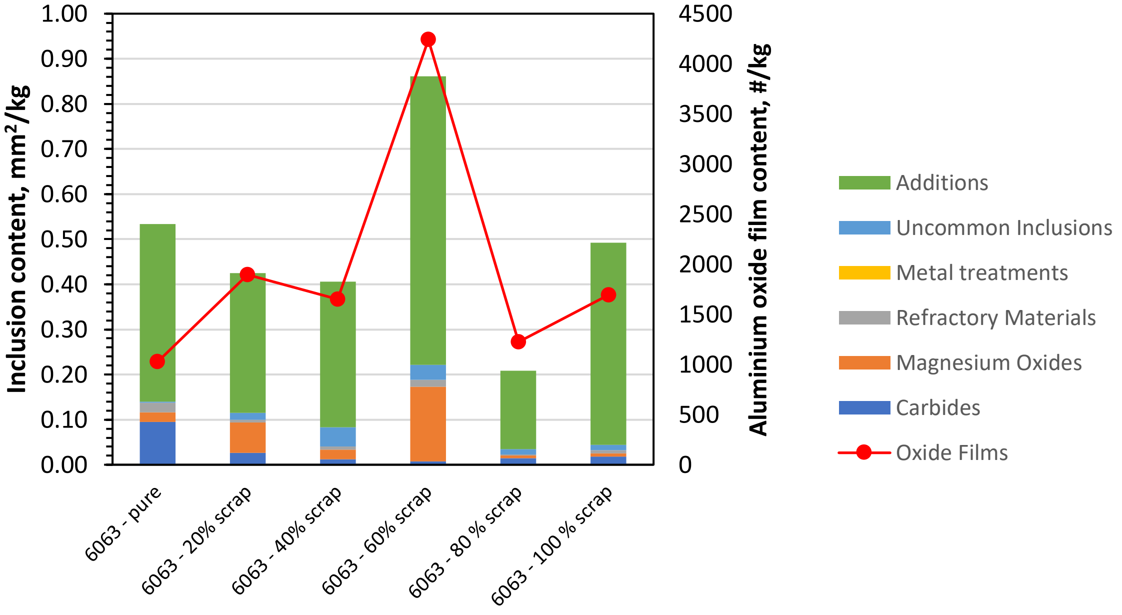

Figure 38. Histogram of Results: Quantification of each inclusion identified for samples 15-20

3.2.3. Microstructure observed

Light Optical Migrographs corresponding to the produced ingots are presented in Figure 39 (low magnification) and Figure 40 (higher magnification). The microstructure overall shows a typical solidification structure composed of alpha grains surrounded by low melting point constituents, segregated to the grain boundaries.

Samples corresponding to 20 % and 40 % scrap appear to show denser population of precipitates. However, this finds no correspondence in neither chemical composition nor presence of inclusions, and therefore could be related to differences in thermal history.

The project has received funding from the European Union's Horizon 2020 research and innovation programme under grant agreement No 101003785

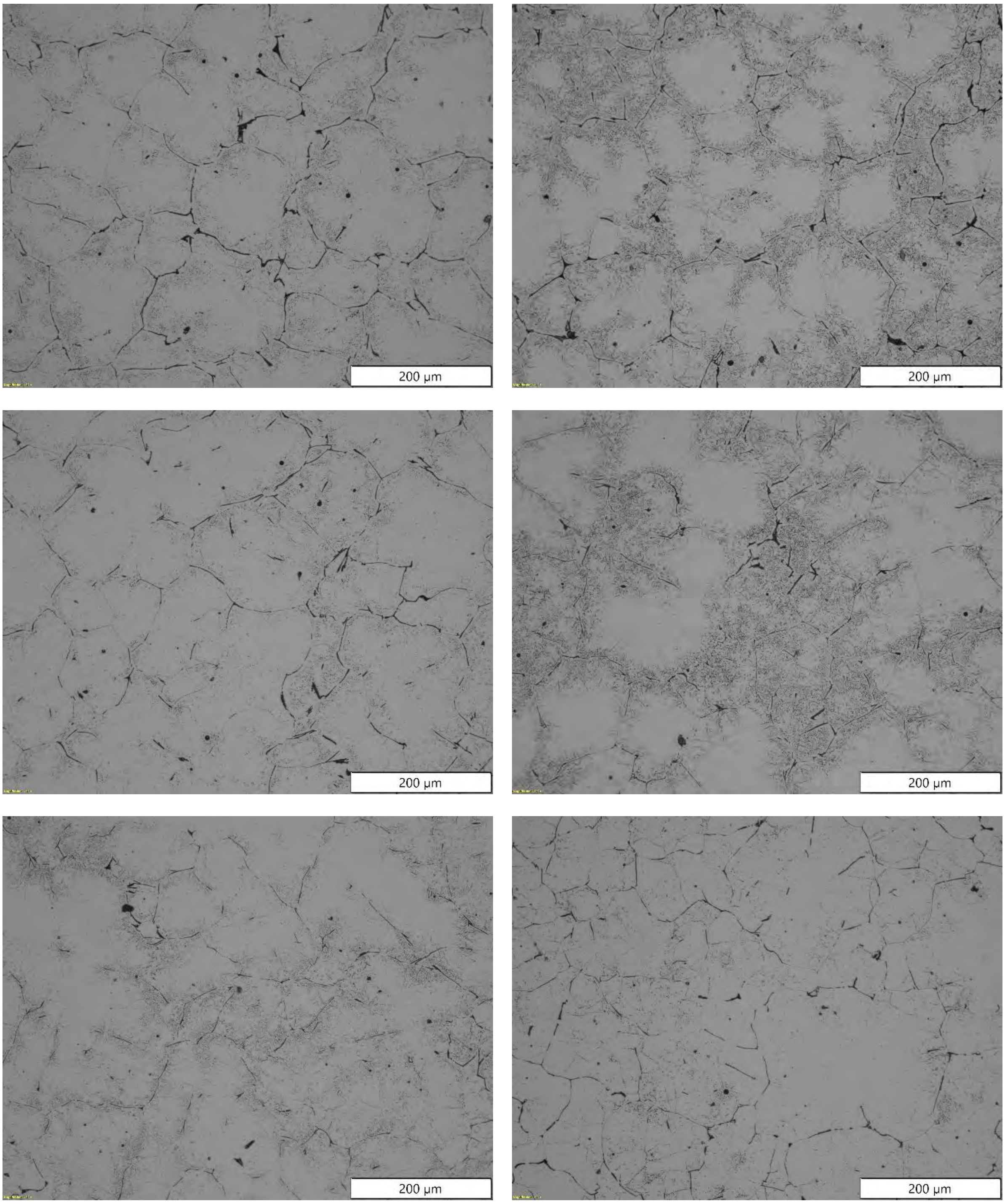

Figure 39. Low magnification microstructure of the 6063 alloy produced with different scrap content: top left 0%, top right 20%, medium left 40%, medium right 60%, bottom left 80% and bottom right 100%.

The project has received funding from the European Union's Horizon 2020 research and innovation programme under grant agreement No 101003785

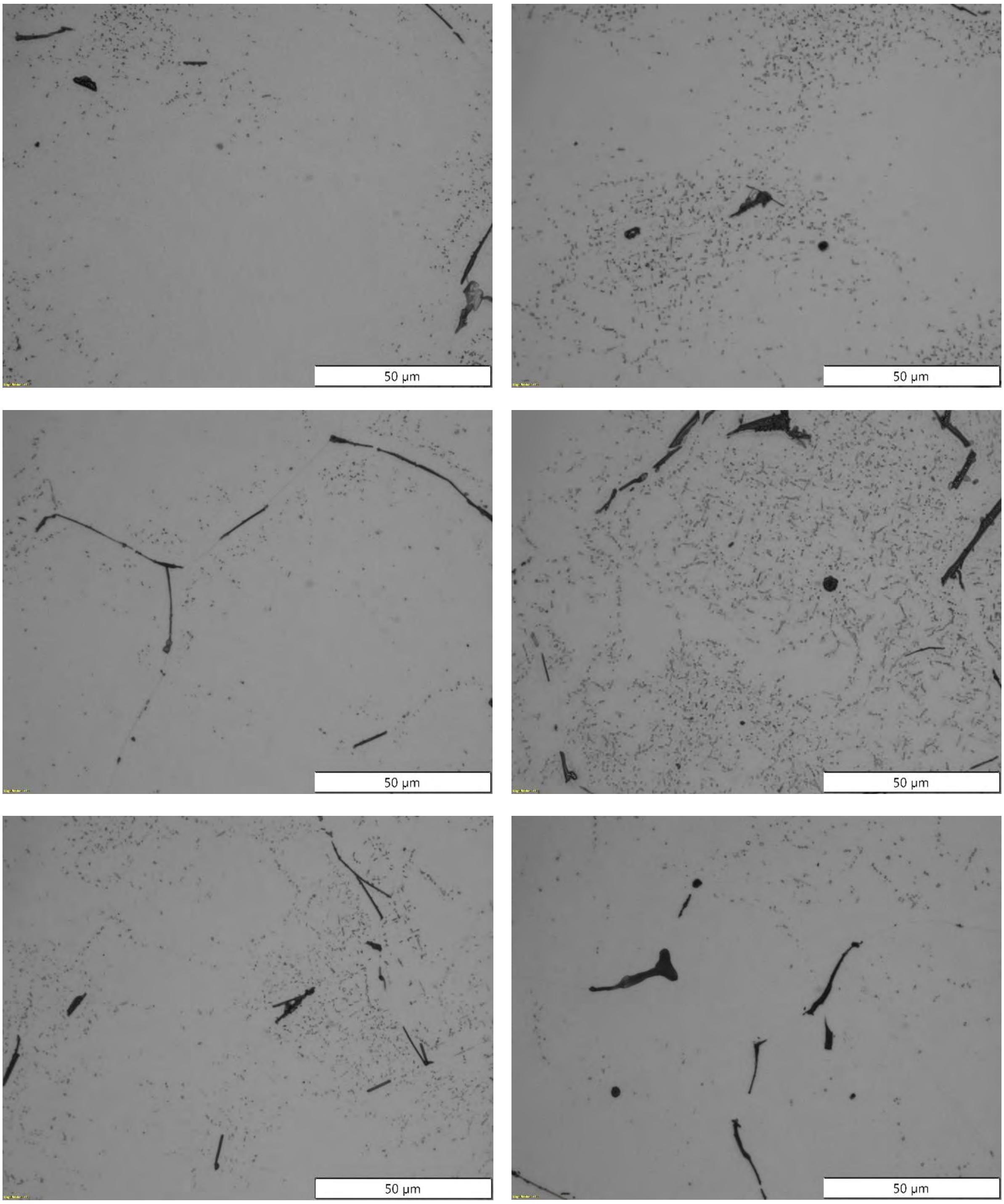

Figure 40. High magnification microstructure of the alloy variant with 0.3% of Mg, produced with different scrap content: top left 0%, top right 20%, medium left 40%, medium right 60%, bottom left 80% and bottom right 100%.

3.2.4. Tensile tests

Tensile tests were performed on as cast material – results are presented in Table 20. Results are well below the typical resistance of extruded and heat treated 6063 but this is to be expected, as the material has not been plastically formed nor heat treated. Nonetheless, one interesting appreciation

The project has received funding from the European Union's Horizon 2020 research and innovation programme under grant agreement No 101003785

can be extracted from the noticeably higher ductility of 80 % scrap samples: this can be related to the remarkable cleanliness found in this batch of material (Figure 38).

Material	σ_{ys} [MPa]	σ_{UTS} [MPa]	A_{25} [%]
6063	73	137	6.3
6063 + 20 % scrap	56	120	8.5
6063 + 40 % scrap	69	125	6.9
6063 + 60 % scrap	52	101	6.5
6063 + 80 % scrap	50	117	13.4
100 % scrap	69	133	8.4

Table 20: Values of the material Yield Strength (σys [MPa]), Ultimate Tensile Strength (σUTS [MPa]) and Elongation at Break (A25 [%]) obtained from the tensile tests for the different scrap ratio configuration

3.2.5. Compression tests

To evaluates the behaviour of the aluminium in extrusion conditions, hot compression tests were performed. Cylindrical samples 8 mm in diameter and 12 mm in length were extracted from the ingots and compressed in an Instron 5582 universal testing machine at a temperature of 500 ± 5 ºC. Samples were heated for 15 minutes before testing, and the test was conducted as crosshead speeds of 250 and 450 mm/min until reaching 60 % deformation. All contact points between the samples and the testing equipment were lubricated. Results are presented in Figure 41 and Table *21* (250 mm/s) and Figure 42 and Table *22* (450 mm/s).

As in previous studies, results show no significant differences between the different sample groups, with almost identical results in 250 mm/min and showing variability but no clear trend at 450 mm/min.

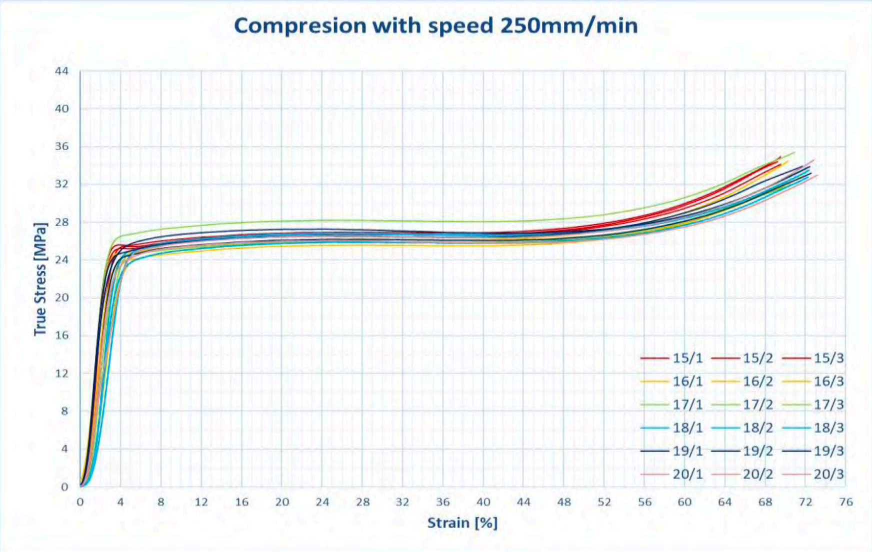

Figure 41. True stress-strain curves from compression test with crosshead speed 250mm/min.

scrap content	Rp0,2 [MPa]	Rp0,5 [MPa]	A_{total} [%]	Rrmax [MPa]

0% scrap	23,5	25,4	68,9	35,2
20% scrap	22,0	23,9	70,6	34,1
40% scrap	23,3	25,1	70,8	34,5
60% scrap	22,7	24,5	70,6	33,9
80% scrap	22,2	24,1	71,9	34,2
100% scrap	21,6	23,6	72,4	34,6

Table 21: Compression results with crosshead speed 250 mm/min (average of 3 samples)

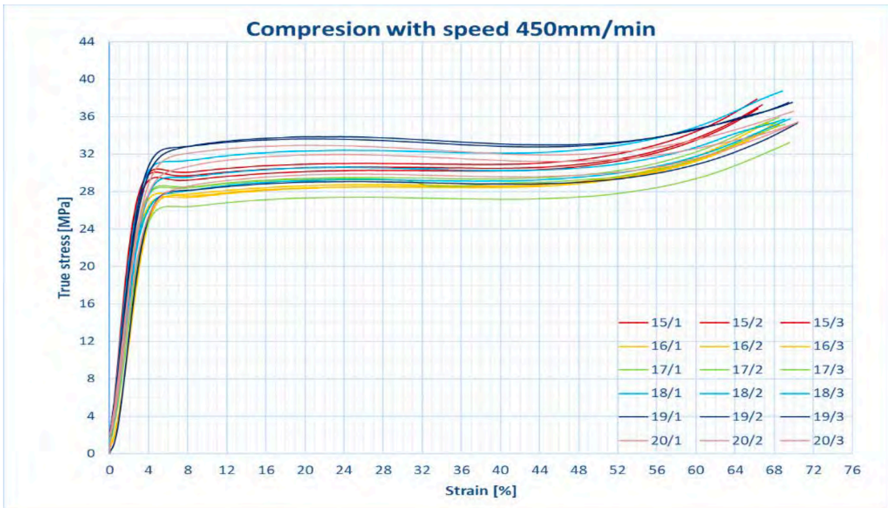

Figure 42. True stress-strain curves from compression test with crosshead speed 450mm/min.

scrap content	Rp0,2 [MPa]	Rp0,5 [MPa]	A_{total} [%]	Rrmax [MPa]
0% scrap	26,0	28,7	66,4	37,4
20% scrap	24,2	26,5	68,2	35,4
40% scrap	24,3	26,7	69,1	34,8
60% scrap	25,1	27,8	69,2	36,8
80% scrap	25,7	28,7	69,9	36,8
100% scrap	24,6	27,4	70,3	35,8

Table 22: Compression results with crosshead speed 450 mm/min (average of 3 samples)

The project has received funding from the European Union's Horizon 2020 research and innovation programme under grant agreement No 101003785

3.3. Comments and remarks

The series of experiments performed on 6063 shows that it was possible to increase stepwise the amount of recycled material on a high quality alloy without significant deviations in composition or negatively affecting the cleanliness of the alloy.

In terms of mechanical properties, samples with different scrap rates performed similarly, both in room conditions and in hot compression.

4. Laboratory trials with stamping alloys

4.1. Experimental methodology

4.1.1. Feedstock and materials used in the trials

Alloys and material format supplied by Profilglass

Profilglass supplied commercial 6181A and 5754 alloy sheets, 2 mm thick, cut in 900 mm x 500 mm blanks (Figure 43). Chemical composition, as reported in the certification sheet, is shown in Table 23.

Figure 43: Pallets loaded with sheet aluminium

	%Si	% Fe	%Cu	%Mn	%Mg	%Cr	Ti	%Zn
5754 (H111)	0.1362	0.2585	0.0166	0.1606	2.8649	0.0098	0.0119	0.0119
6181A (T4)	0.9120	0.2733	0.1410	0.2997	0.7574	0.0206	0.0283	0.0590

Table 23: Chemical composition reported in the certificate sheets received from Profilglass

Scrap used to mix with reference material

As 5xxx fraction of COMET scrap was wrongly sorted, Profilglass provided some 5xxx scrap to Eurecat, to be used it in WP1 to produce 5754 alloy. About 70 kg of scrap of mixed 5xxx series alloys were provided (Figure 33). With a general sight it was clear that all the scrap supplied was exclusively aluminium sheet, but of different thicknesses. A selection of 10 representative pieces were taken from the container to have a precise chemical analysis of them.

The project has received funding from the European Union's Horizon 2020 research and innovation programme under grant agreement No 101003785

Figure 44: Picture of the 2 boxes containing the 5xxx aluminium scrap (left) and detail showing the scrap present in them (right)

The results of the chemical analysis of the 10 selected parts are presented in Table 16. It can be observed that most of the pieces belong to 5xxx series, as expected. However, there are 3 of the pieces that are 6xxx series alloys. So, at a much lower ratio than in the scrap provided by COMET and characterized in Deliverable 1.2, but this 5xxx scrap is also mix up with some pieces from 6xxx alloys.

n=5	%Si	% Fe	%Cu	%Mn	%Mg	%Cr	%Ni	%Zn	Alloy
Spec 1	0.31	0.39	0.06	0.23	2.90	0.03	<0.03	0.03	5754
Spec 2	0.88	0.27	0.09	0.16	0.40	0.05	<0.03	<0.03	6082
Spec 3	0.23	0.31	0.03	0.19	1.96	0.08	<0.03	<0.03	5051
Spec 4	0.88	0.24	0.1	0.16	0.42	0.04	<0.03	0.03	6082
Spec 5	0.12	0.24	0.08	0.38	4.45	<0.03	<0.03	<0.03	5182
Spec 6	0.31	0.41	0.05	0.28	3.00	0.03	<0.03	0.03	5754
Spec 7	0.98	0.26	0.09	0.16	0.36	0.04	<0.03	<0.03	
Spec 8	0.22	0.31	0.03	0.25	1.94	0.08	<0.03	<0.03	5051
Spec 9	0.09	0.30	0.03	0.33	3.90	<0.03	<0.03	<0.03	5042
Spec 10	0.07	0.25	0.04	0.32	4.18	<0.03	<0.03	<0.03	5182

Table 24: Chemical composition measured by spark OES with SPECTROMAXx equipment on the 3 fragments selected from the 5xxx metal sheet supplied by Profilglass

For 6181 alloy it was used the 6063 scrap from extrusion alloys, correcting the Si and Mg content with the addition of master alloys to correct the lower amount of these elements present in 6063 alloy.

The project has received funding from the European Union's Horizon 2020 research and innovation programme under grant agreement No 101003785

4.2. Results obtained from the produced samples

4.2.1. Chemical composition of the different batches

As in the use cases for High Pressure Die Casting and Extrusion, sample ingots were produced using the materials provided by Profilglass (Figure 43), increasingly mixed with the scrap described in Figure 44 and Table 24 for 5754 alloy and in Figure 33 and Table 16 for 6181 alloy. When introducing scrap, chemical composition was corrected by adding alloying elements, considering the average chemical composition of each of the scrap types.

Material was produced in the form of ingots (Figure 45 a) and plates identical to those previously cast in HPDC materials (Figure 4). Plates were then machined to produce approximately prismatic feedstock that could be used for laboratory analysis (Figure 45 b and c).

a)

b)

c)

Figure 45: Ingots cast using the sheet metal compositions with increasing scrap contents: a) as-cast ingot; b) and c) samples machined from a plate of 5754 and 6181 with scrap contents 0%, 20%, 40%, 60%, 70% and 100%.

The project has received funding from the European Union's Horizon 2020 research and innovation programme under grant agreement No 101003785

Chemical analysis was performed in the middle section of the ingot. Results are reported in Table 25 (5754-based casts) and Table 26 (6181-based casts). Chemical analysis of the original sheet, as measured by the SPECTROMAXx spectrometer available at Eurecat is provided for reference.

For 5754, the main alloying elements fall within acceptable limits inside the whole range of trials, with the following observations:

- Increase in Manganese is the main risk, as this element comes from the used scrap. However, this increase is only moderate, and even in 100 % scrap cases values are fairly low (0.23%).
- Silicon increases is also a relevant issue; becoming higher than the standard at the 60 % scrap cast. The problem may come from the presence of 6xxx scrap mixed with the 5xxx scrap provided by Profilglass. As can be seen in Table 24, the 5xxx scrap is misxed with 6xxx series scrap, which has a much higher amount of Si. Therefore this deviation can be corrected by improving the scrap sorting method.
- Mg decreases as scrap is included. This is also related to the uncertainty of the scrap composition. 6xxx alloys have a lower Mg content than 5xxx and, therefore, reduce the total content of Mg present in the scrap.
- Fe and Cu increase only moderately
- Cr, Zn, Ti: no significant increase for these trace elements, thanks to correct selection of scrap.

n=5	%Si	% Fe	%Cu	%Mn	%Mg	%Cr	%Zn	%Ti
EN-573-3	0.25	0.40	0.1	0.5	2.6-3.6	0.3	0.2	0.15
Initial sheet	0.15	0.27	0.02	0.15	2.79	<0.03	<0.03	<0.03
0% scrap	0.18	0.29	0.02	0.16	2.78	<0.03	<0.03	<0.03
20% scrap	0.23	0.28	0.03	0.18	2.72	<0.03	<0.03	<0.03
40% scrap	0.25	0.26	0.04	0.19	2.66	<0.03	<0.03	<0.03
60% scrap	0.35	0.28	0.06	0.21	2.49	<0.03	<0.03	<0.03
80% scrap	0.39	0.27	0.06	0.22	2.44	<0.03	<0.03	<0.03
100% scrap	0.43	0.28	0.07	0.23	2.37	<0.03	<0.03	<0.03

Table 25: Chemical composition of the different 5754-based casts with increasing scrap content. Composition as published in standard EN-573-3 is included for reference

For 6181, the main alloying elements fall within acceptable limits inside the whole range of trials, with the following observations:

- Increase in Manganese and Silicon is the main risk, as this element comes from the used scrap. However, this increase is only moderate, and even in 100 % scrap cases values are fairly low (0.23%).
- Silicon increase is a relevant issue. This time Silicon was manually added (not coming from the scrap), as 6063 alloy has a lower content of Si than 6181and this deviation can be improved through better composition control.
- Mg decreases as scrap is included; this can be solved also with better correction of the final alloy adjustment as described above
- Fe, Zn and trace ements Cr, Ti don't increase significantly.

The project has received funding from the European Union's Horizon 2020 research and innovation programme under grant agreement No 101003785

n=5	%Si	% Fe	%Cu	%Mn	%Mg	%Cr	%Ni	%Zn	%Ti
Initial sheet	0.85	0.29	0.13	0.30	0.76	<0.03	<0.03	0.06	<0.03
0% scrap	0.88	0.32	0.13	0.29	0.74	<0.03	<0.03	0.06	<0.03
20% scrap	0.92	0.33	0.11	0.25	0.76	<0.03	<0.03	0.08	<0.03
40% scrap	0.95	0.32	0.10	0.22	0.71	<0.03	<0.03	0.08	<0.03
60% scrap	0.96	0.29	0.06	0.14	0.68	<0.03	<0.03	0.08	<0.03
80% scrap	1.00	0.27	0.05	0.10	0.66	<0.03	<0.03	0.08	<0.03
100% scrap	1.07	0.26	0.03	0.06	0.65	<0.03	<0.03	0.08	<0.03

Table 26: Chemical composition of the different 6181-based casts with increasing scrap content

As a conclusion, the main deviations in chemical composition can be improved with a better scrap sorting and control techniques and melt composition control, which resulted in excessive addition of some alloying elements (Si) and too short addition of Mg.

4.2.2. Microstructure observed

The microstructure was observed in samples extracted from the various ingots. It must be noticed that the results correspond to as-cast material, and therefore is not relevant for sheet metal: this would require several steps of hot rolling, cold rolling and annealing to generate the desired texture. However, this analysis is still valid to evaluate the presence of unexpected phases in the material.

As a complementary work, selected samples were hot worked by heating them to full solubilization (530 ºC) and compressing them in a hydraulic press into approximately 50 % reduction (Figure 46 a). For 5754, the resulting samples were then cold pressed, to a 30% reduction (Figure 46 b), following Snopinski et al in *Materials 2020, 13, 301; doi:10.3390/ma13020301*.

a)

b)

Figure 46: Plastic formed ingots: a) 5754 and b) 6181

The project has received funding from the European Union's Horizon 2020 research and innovation programme under grant agreement No 101003785

Microstructures obtained from the sheet metal show silicon-based polygonal particles in a mainly alpha matrix. Grain boundaries are not very easily revealed using the common etchants, as this results on over etching in the particles; nevertheless, micrographs suggest slightly elongated grains as expected in cold rolled material (top images in Figure 47 for 5754 and Figure 48 for 6181).

As-cast ingots show a reticular structure, composed by low-melting point phases surrounding alpha grains, suggesting a slightly dendritic microstructure with non-alpha phases segregated in the grain boundaries in eutectic-like formations. This structure and phase composition is repeated for all scrap amounts and in both 5754 (Figure 47, left column) and 6181 (Figure 48, left column). It is noteworthy to comment that the amount of scrap does not seem to have an impact on the structure or presence of phases.

Deformed samples show how plastic forming and recovery mechanisms have broken the as-cast structure. Clearly elongated grains can be recognized, particularly for 5754 alloy. However, the overall microstructure still presents a high degree of segregation, with silicon-based particles concentrating in the alpha-grain boundaries. In this regard, hot forming experiments have not accomplished to generate a microstructure comparable to the rolled material used as reference. However, the deformed sample still show no significant difference in phases or distribution among the samples with different percentage of scrap.

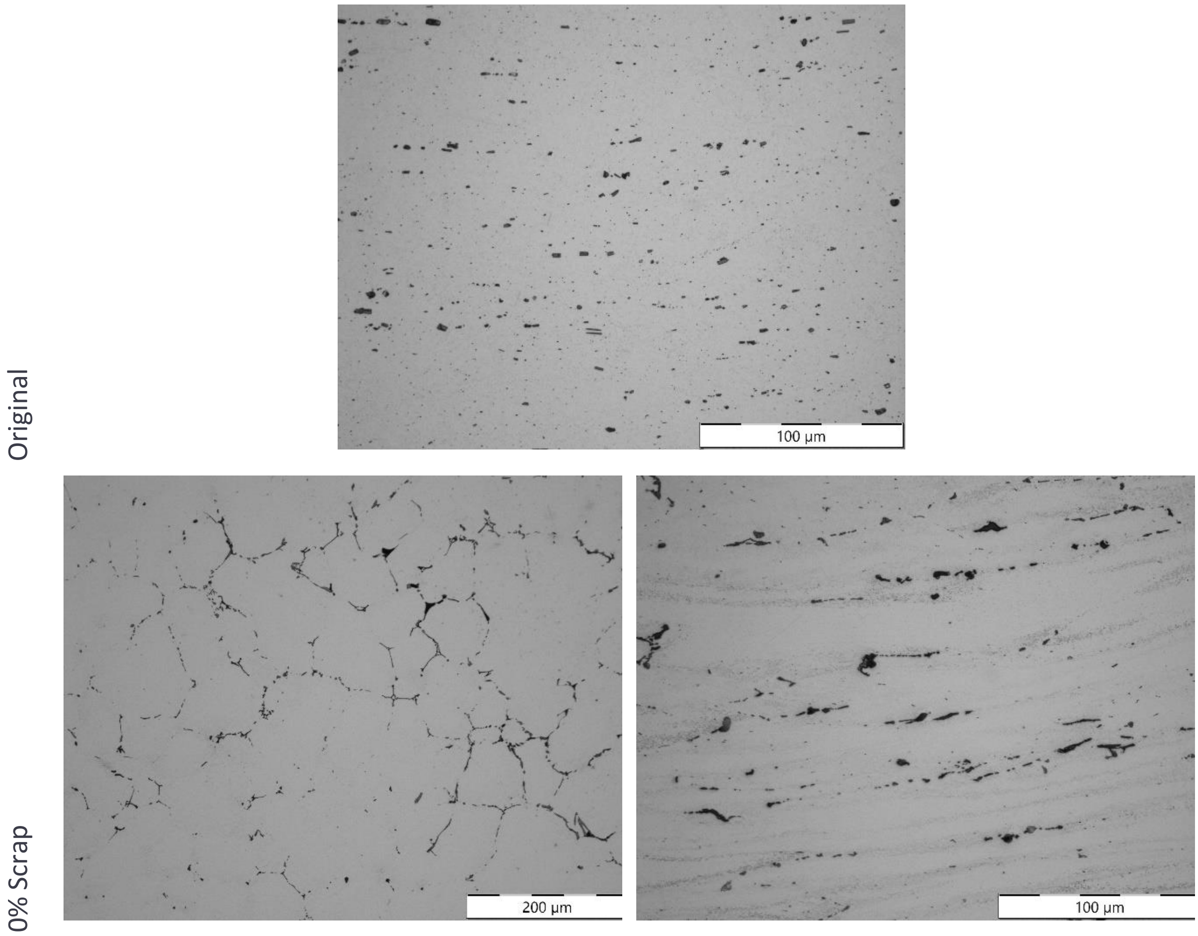

The project has received funding from the European Union’s Horizon 2020 research and innovation programme under grant agreement No 101003785

40% Scrap

100% Scrap

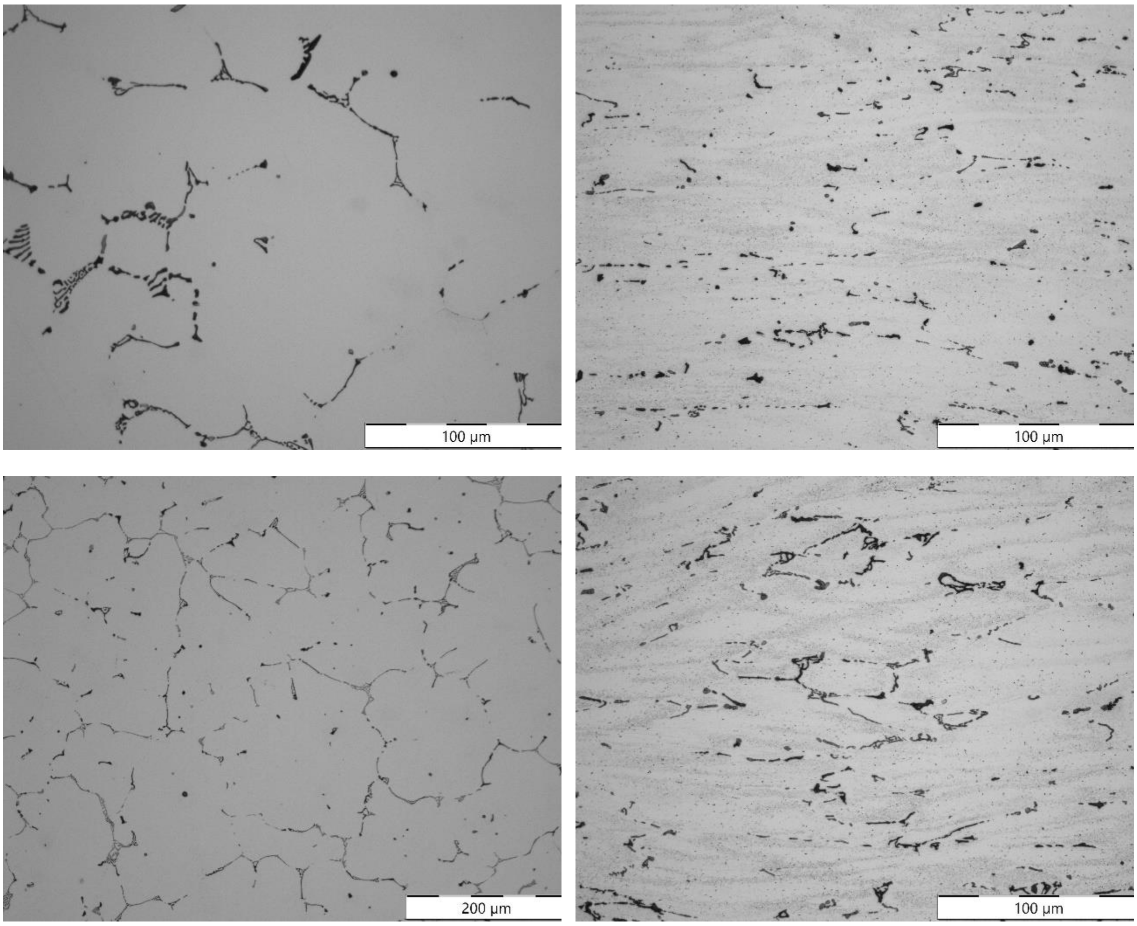

Figure 47: Microstructures corresponding to 5754 material with selected scrap compositions; left: as-cast ingots and right: plastically formed material

Original

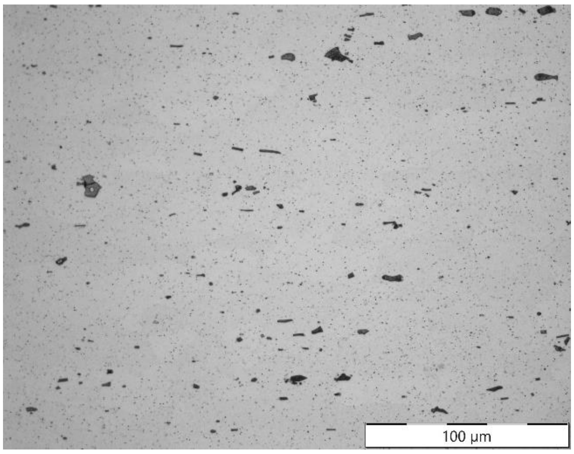

The project has received funding from the European Union's Horizon 2020 research and innovation programme under grant agreement No 101003785

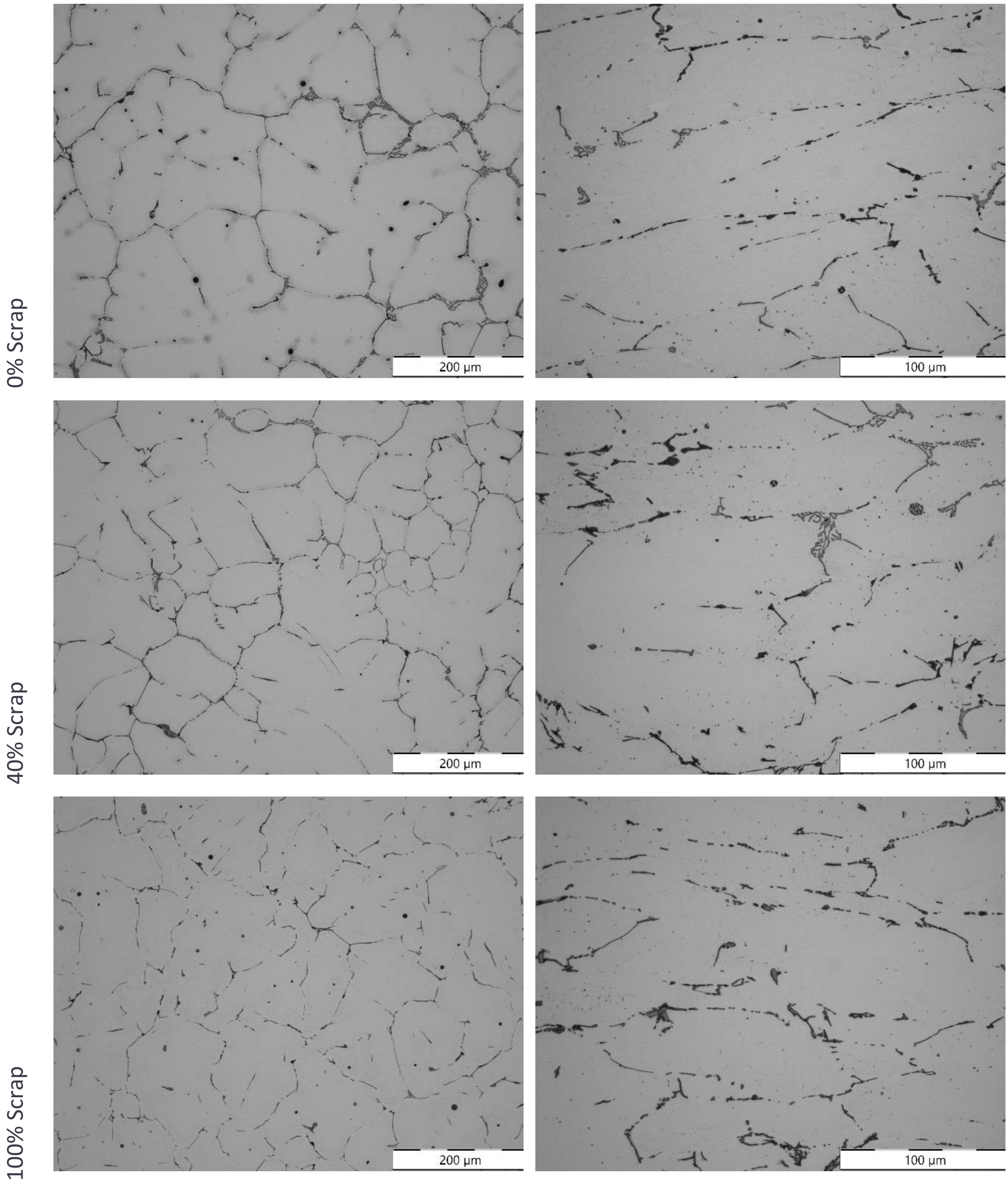

Figure 48: Microstructures corresponding to 6181 material with selected scrap compositions; left: as-cast ingots and right: plastically formed material

4.2.3. Mechanical properties

While it was initially considered to perform tensile tests on these materials, the investigations on microstructure showed that the material properties would be hugely different from what could be expected in rolled material. Indeed, hot plastic deformation generates phenomena including texture, closing of pores and defects, and recrystallization and recovery that confer sheet metal its

The project has received funding from the European Union's Horizon 2020 research and innovation programme under grant agreement No 101003785

characteristic mechanical properties. This is particularly critical for strain hardening 5754 alloy, which derives its performance from the microstructure generated during rolling, and in the cold rolling steps in particular.

While forging experiments showed that it was possible to obtain a microstructure approaching that of a wrought material, sheet metal samples cannot be obtained without rolling. However, it was possible to obtain Hardness measurements to check whether the alloys presented properties in the expected range.

For 5754 (Table 27), Hardness differences found in the first step (hot working) could be related to the different reduction applied; this was a limitation of the test equipment.

However, significant hardening was observed after cold working for a similar 65% reduction: the different samples showed similar maximum hardness (94-95 HV1) after cold work. This fits very well with the expected behaviour of the material, particularly sensitive to strain hardening.

	Hot formed				Cold Worked		
	Thickness (initial, mm)	Thickness (final, mm)	%reduction	HV1	Thickness (final, mm)	%reduction	HV1
0%	15,11	9,94	35%	71 ± 3	3.39	66%	94± 3
40%	15,53	10,00	35%	71 ± 3	3.29	67%	94± 3
100%	11,74	6,51	45%	85 ± 3	2.40	64%	95± 3

Table 27: Mechanical properties measured on 5754 ingots, after hot forming and after cold work; HV1

In the case of 6181 ingots (Table 28), a sample heat treatment was applied consisting in quenching after rolling, and aging for 1h at 200 ºC. This heat treatment was not optimized, as seen in the relatively low hardness values obtained (85 HV as opposed to the expected >100 HV), but shows that the three samples responded similarly well to the treatment.

As a trend, a small reduction in hardness is observed with increasing scrap %. While this could be related to the decreasing amount of Magnesium in the ingots, it must be noticed that the difference in values is not large enough to ensure that this trend goes beyond measurement uncertainty. Moreover, the overly manual process implies that samples have received differences in thermomechanical history.

	Thickness (initial, mm)	Thickness (final, mm)	%Reduction	Treatment	HV1
0%	11.98	6.88	42%	1h 200ºC	86± 3
40%	10.6	6.91	35%	1h 200ºC	84± 3
100%	11.42	6.4	44%	1h 200ºC	82± 3

Table 28: Mechanical properties measured on 6181 ingots after a sample T6 treatment

4.3. Comments and remarks

The two main concerns in the use of recycled material in aluminium alloys are ensuring the chemical composition, on the one hand, and control over the presence of inclusions and foraneous particles. This is a common issue with the other studied processes, but it is worth considering their implications on sheet metal:

The project has received funding from the European Union's Horizon 2020 research and innovation programme under grant agreement No 101003785

From the **chemical composition** point of view, the impact on formability is paramount. As opposed to die casting and extrusion, sheet metal is subject to severe plastic forming in room temperature conditions. In this sense, the excess of some alloying elements (Zn, Cu, Mn) has a direct impact on formability, and needs to be actively corrected in the composition. The experiences in this task have shown that this is possible, provided that accurate scrap sorting can be performed.

Indeed, the largest deviations have been found in manually added alloying elements (Si, Mg): this is easily improved in an industrial installation with melt composition controls.

From the **inclusions** point of view, extraneous particles have a deleterious effect on alloy cold formability, as well as on fracture toughness, as an indirect predictor of severe plastic forming operations (such as hole expansions). Micrograph-based analysis did not show significant increase in the presence of particles. This will need to be verified in future Footprinter analyses analogous to those performed for casting and extrusion alloys.

5. Conclusions and Outlook

The present document summarizes the main results obtained in Task 1.3 of SALEMA project, assessing the effect that the use of different amount of scrap has on the microstructure and mechanical properties of the partially recycled aluminium alloys selected for 3 different processes: HPDC, extrusion and stamping. The main conclusions that can be inferred from the results obtained are:

High Pressure Die Casting:

- In general, the use of scrap affects the quantity of inclusions present in the melt and retained in the Prefil Footprinter® filter. The main increment is produced by a higher concentration of oxides, which could be easily removed from the melt with a melt cleaning treatment.
- The higher quantity of particles presents in the materials produced with scrap leads to a reduction of the flowability of the melt
- The Mg level of AlSi10MnMg alloys affects mechanical resistance. The higher the Mg content, the higher the yield strength and ultimate tensile strength of the material
- Low and high magnification optical microscope images obtained for all the alloys do not reveal significant changes, neither in grain size or SDAS, nor in intermetallic particles varies with the amount of scrap present

Extrusion

- In the case of extrusion alloy 6063, it was possible to increase scrap content without negatively affecting the cleanliness of the alloy.
- Alloy 6063 reached excessive level of Silicon. This could be traced to furnace contamination, originating on residues of previous HPDC alloy trials.
- All this points that, even with careful scrap sorting, it is necessary to monitor melt composition to account for scrap variability.

Sheet Metal

The project has received funding from the European Union's Horizon 2020 research and innovation programme under grant agreement No 101003785

- Using carefully selected scrap, it is possible to maintain satisfactory chemical composition even in alloys with low amount of alloying elements, such as the 6063 extrusion alloy and 5754 and 6181 sheet metal. In this regard, the following issues were detected:
- The increase in content of common alloying elements or scrap contaminants, such as Fe, Cu and Mn, was successfully avoided in all cases.
- Alloy 5754 ended showing excessive Silicon, due to the use of misidentified 6000-series scrap.
- Alloy 6181 reached excessive level of Silicon. In this case, Si additions had been manually introduced to the melt to correct the calculated composition.

The project has received funding from the European Union's Horizon 2020 research and innovation programme under grant agreement No 101003785

6. ANNEX Quality certificates

1. Chemical composition of AlSi10MnMg provided by Raffmetal

ALLOY	Alsi10MnMg	Alsi10MnMg	Alsi10MnMg
CASTING N°	10277/21	10281/21	10282/21
Cu	0,021	0,008	0,023
Mg	**0,181**	**0,281**	**0,437**
Si	10,578	10,148	10,237
Fe	0,139	0,146	0,182
Mn	0,596	0,494	0,535
Ni	0,005	0,004	0,005
Zn	0,012	0,01	0,016
Pb	0,003	0,002	0,003
Sn	0,001	0,001	0,001
Ti	0,062	0,032	0,06
Cr	0,005	0,004	0,006
Sb	0,0004	0,0001	0,0017
Ga	0,0093	0,0103	0,012
V	0,0098	0,009	0,0076
Sr	0,0273	0,029	0,0143
P	0,0005	0,0012	0,0008
Na	0,0001	0,0001	0,0001
Bi	0,0006	0,0006	0,0007
Be	0,0001	0,0001	0,0001
Li	0,0001	0,0001	0,0001
Zr	0,0008	0,0005	0,0008
Cd	0,0001	0,0001	0,0001
Co	0,0002	0,0002	0,0002
B_	0,0001	0,0001	0,0001
Ca	0,002	0,0011	0,0015
Hg	0,0001	0,0001	0,0001
As	0,0009	0,0008	0,0009

2. Chemical composition of the aluminium alloy 6063 provided by ASAS

Si	Fe	Cu	Mn	Mg	Zn	Ti	Cr	Al
0,566	0,173	0,017	0,036	0,531	0,019	0,018	0,009	Remainder

The project has received funding from the European Union's Horizon 2020 research and innovation programme under grant agreement No 101003785

3. Profilglas certificate

Extract of quality cerfificate corresponding to 5754 sheet

Description of the product BA5S2000HA10900005000MNB Chapa 5754-A 2 H111 900 x 500 MF -0,06

Alloy	Thick.	Temper	Width	Length	Fin.	Tol.	Prot.
5754-A	2	H111	900	x 500	MF	neg.	

Mechanical Properties

Rp0,2 MPa	Rm MPa	A50mm%	A5mm%
136,28	214,04	21,49	25,50

Chemical Composition (%) (EN-573-3)

Si	Fe	Cu	Mn	Mg	Cr	Zn	Ti	Al
0,1362	0,2585	0,0166	0,1606	2,8649	0,0098	0,0039	0,0119	96,5010

Extract of quality cerfificate corresponding to 6181A sheet

Description of the product BA6L2000T041150005000MCBB06468+534475 Chapa 6181A 2 T4 1150 x 500 MF T+/-0,05

Alloy	Thick.	Temper	Width	Length	Fin.	Tol.	Prot.
6181A	2	T4	1150	x 500	MF	cent.	

Chemical Composition (%) (EN-573-3)

Si	Fe	Cu	Mn	Mg	Cr	Zn	Ti	Al
0,9120	0,2733	0,1410	0,2997	0,7574	0,0206	0,0590	0,0283	97,4702

The project has received funding from the European Union's Horizon 2020 research and innovation programme under grant agreement No 101003785